Complex Effects of Putative DRP-1 Inhibitors on Stress Responses in Mouse Heart and Rat Cardiomyoblasts

Lauren Wendt, Jelena Vider, Louise E. See Hoe, Eugene Du Toit, Jason N. Peart and John P. Headrick

School of Medical Science, Griffith University, Southport Q 4217 AUSTRALIA (L.W., J.V., E.D.T., J.N.P., J.P.H) and Critical Care Research Group, The Prince Charles Hospital and The University of Queensland, Chermside, Q 4032, AUSTRALIA (L.E.S.H)

Abbreviations: BAX, BCL2 associated X; BCL2, B-cell lymphoma 2; DRP-1, dynamin-related protein-1; I-R, ischemia-reperfusion; LC3B, microtubule associated protein 1 light chain 3b; MDIVI-1, mitochondrial division inhibitor 1; mPTP, mitochondrial permeability transition pore; MTT, 3-(4,5-dimethylthiazol-2-yl)-2,5-diphenyltetrazolium bromide; OPA-1, optic atrophy-1; PARP, poly-(ADP-ribose) polymerase; RISK, reperfusion injury salvage kinase; ROS, reactive oxygen species; TMRM, tetramethylrhodamine methyl ester perchlorate.

Running Title: DRP-1 Inhibitors and Cardioprotection

Corresponding Author:
Prof. John P. Headrick
School of Medical Science
Griffith University
Southport QLD 4217
AUSTRALIA
Ph: +61 7 55528292
FAX: +61 7 55528802
E-mail: J.Headrick@griffith.edu.au

Manuscript Information:

Text Pages – 21
Tables - 2
Figures – 11 + 3 Supplemental figures
References – 81

Word Count:

Abstract – 250 words
Introduction – 498 words
Discussion - 2162 words

Section Assignment: Cardiovascular

ABSTRACT

Dynamin-related protein-1 (DRP-1) dependent mitochondrial fission may influence cardiac tolerance to ischemic or oxidative stress, presenting a potential 'cardioprotective' target. Effects of dynamin inhibitors MDIVI-1 and dynasore on injury, mitochondrial function and signaling proteins were assessed in distinct models: ischemia-reperfusion (I-R) in mouse hearts, and oxidative stress in rat H9c2 cardiomyoblasts. Hearts exhibited substantial cell death (~40 IU LDH efflux) and dysfunction (~40 mmHg diastolic pressure, ~40% contractile recovery) following 25 min ischemia. Pre-treatment with 1 μM MDIVI-1 reduced dysfunction (30 mmHg diastolic pressure, ~55% recovery) and delayed without reducing overall cell death, whereas 5 μM MDIVI-1 reduced overall death while paradoxically exaggerating dysfunction. Post-ischemic expression of mitochondrial DRP-1 and phospho-activation of ERK1/2 were reduced by MDIVI-1. Conversely, 1 μM dynasore worsened cell death and reduced non-mitochondrial DRP-1. Post-ischemic respiratory fluxes were unaltered by MDIVI-1, although a 50% fall in complex-I flux control ratio was reversed. In H9c2 myoblasts stressed with 400 μM H_2O_2, treatment with 50 μM MDIVI-1 preserved metabolic (MTT assay) and mitochondrial (basal respiration) function without influencing survival. This was associated with differential signaling responses, including reduced early *vs*. increased late phospho-activation of ERK1/2, increased phospho-activation of AKT, and differential changes in determinants of autophagy (reduced LC3B-II/I *vs.* increased Parkin) and apoptosis (reduced PARP cleavage *vs*. increased BAX:BCL2). These data show MDIVI-1 (not dynasore) confers some benefit during I-R/oxidative stress. However, despite mitochondrial and metabolic preservation, MDIVI-1 exerts mixed effects on cell death *vs*. dysfunction, potentially reflecting differential changes in survival kinase, autophagy and apoptosis pathways.

Significance

Inhibition of mitochondrial fission is a novel approach to still elusive cardioprotection. Assessing effects of fission inhibitors on responses to ischemic or oxidative stress in hearts and cardiomyoblasts reveals MDIVI-1 and dynasore induce complex effects and limited cardioprotection. This includes differential impacts on death and dysfunction, survival kinases and determinants of autophagy and apoptosis. While highlighting the interconnectedness of fission and these key processes, results suggest MDIVI-1 and dynasore may be of limited value in the quest for effective cardioprotection.

Introduction

Mitochondrial phenotype governs cellular to systemic health, and lies at the cross-roads of cell survival and death. Unsurprisingly, adaptive quality control mechanisms have evolved, including dynamic fusion-mediated elongation *vs*. fission-mediated fragmentation. This cycle contributes to maintenance of mitochondrial health in long-lived cardiomyocytes and neurons. Evidence of dysregulation with aging and disease has focused attention on fusion and fission as potential therapeutic targets (Ong and Hausenloy, 2010; Biala *et al.*, 2015; Dorn, 2015). Fission is governed by dynamin-related protein (DRP-1) and fission 1 homologue protein (FIS1), and dynamin GTPase inhibitors such as MDIVI-1 (mitochondrial division inhibitor 1) and dynasore (dynamin inhibitor 1) have been tested for benefit (Reddy, 2014). Treatment with 5-50 μM MDIVI-1 reportedly conditions hearts against I-R injury (Ong *et al.*, 2010, Sharp *et al.*, 2014), while post-ischemic protection is evident with 25 μM MDIVI-1 (Sharp *et al.*, 2014). However, important questions remain regarding the cardioprotective utility, mechanisms and selectivity of fission inhibitors (Preta *et al*., 2015; Rosdah *et al.,* 2016; Smith and Gallo 2017).

Despite association of fission and cell death (Frank *et al.*, 2001; Taguchi *et al.*, 2007), underlying roles of dynamism proteins require delineation. This is highlighted by observations that: increased fission fails to initiate death (Chen *et al.*, 2005; Papanicolaou *et al.,* 2012; Song and Dorn, 2015; Song *et al.*, 2015) and improves stress-resistance (Papanicolaou *et al.,* 2012); DRP-1 dependent fission can be anti-apoptotic (Szabadkai *et al.*, 2004); and DRP-1 inhibition/down-regulation may worsen myocardial infarction (Ikeda *et al.*, 2015), post-ischemic necroptosis (Dong *et al.*, 2016) and apoptosis (Zhang *et al.*, 2013). Such outcomes may reflect complex interactions between fission/fission proteins and autophagy (Dorn and Kitsis, 2015; Marin-Garcia and Akhmedov, 2016), survival kinase signaling (Gharanei *et al.,* 2013; Gan *et al.,* 2014; Lim *et al.,* 2015) and cell death pathways (Dorn and Kitsis, 2015; Marin-Garcia and Akhmedov, 2016). Contributions of pleiotropic *vs*. specific dynamism mechanisms

are yet to be resolved. Indeed, cardiac benefits of fusion proteins may be largely pleiotropic in nature (Ong *et al.,* 2017), and there is evidence MDIVI-1 and dynasore induce DRP-1 independent effects at concentrations employed to protect cells (Preta *et al*., 2015; Bordt *et al*., 2017; Smith and Gallo 2017). More fundamentally, active mitochondrial dynamism is not a feature of cardiomyocytes, which are dense with fragmented mitochondria (Song and Dorn, 2015) and may benefit from further fission (Papanicolaou *et al.,* 2012).

We assessed effects of two distinct cell-permeable dynamin inhibitors (**Fig. 1**): MDIVI-1, a quinazolinone reportedly specific for DRP-1 inhibition at ≤25 μM (Smith and Gallo, 2017); and dynasore, a semicarbazone that appears selective for dynamin/DRP-1 GTPase inhibition at ≤80 μM (Macia *et al.,* 2006). Given the conflicting effects of DRP-1 inhibition in different models (Ong and Hausenloy, 2010; Dong *et al.*, 2016), and potential non-specific actions (Preta *et al*., 2015; Smith and Gallo 2017; Bordt *et al*., 2017), we assess impacts on markers of cell injury together with mitochondrial function and regulatory protein expression in 2 distinct models: I-R in mouse hearts, and oxidative stress in rat cardiomyoblasts.

Materials and Methods

Mice and Ethics

Experiments were performed using young (9-12 week) male C57Bl/6J mice. Animals were purchased from the Animal Resources Center (Canning Vale WA, Australia) at 8 wks of age and were habituated to the animal facility for a minimum of 7 days before use. Mice were housed in groups of 4-5, with sawdust bedding and *ad lib* access to water and food throughout all studies. Animals were maintained in an artificial 12-hour day/night lighting cycle (lights on at 07:00) at a constant temperature of 21°C (40% humidity). A total of 50 mice were used, with none excluded from analysis. All investigations were approved in accordance with Animal

Ethics Committee of Griffith University, under the guidelines of "*The Animal Care and Protection Act 2001, section 757*", which is accredited by the Queensland Government, Department of Primary Industries and Fisheries (AEC number MSC/05/13 licensed to Jason N. Peart).

Reagents

The inhibitors MDIVI-1 (PubChem CID: 3825829) and dynasore hydrate (PubChem CID: 136239889) were purchased from Sigma-Aldrich (St. Louis, MO, USA). Drug structures are shown in **Fig. 1**. Dulbecco's modified essential medium (DMEM), fetal bovine serum (FBS) and other tissue culture reagents were obtained from Life Technologies Inc. Tetramethylrhodamine methyl ester perchlorate (TMRM) was purchased from Molecular Probes (Thermo-Fischer Scientific, NJ, USA). All other chemicals were purchased from Sigma-Aldrich.

Perfused Heart Protocol And Experimental Groups

Langendorff perfused hearts were prepared as detailed previously (Peart and Headrick, 2003; Reichelt *et al.*, 2009). Briefly, mice were anesthetized with sodium pentobarbital (60 mg/kg i.p.) and hearts excised and cannulated for Langendorff-perfusion with Krebs–Henseleit buffer (119 mM NaCl, 11 mM glucose, 22 mM $NaHCO_3$, 4.7 mM KCl, 1.2 mM $MgCl_2$, 1.2 mM KH_2PO_4, 1.2 mM EDTA, and 2.5 mM $CaCl_2$) bubbled with 95% O_2/5% CO_2 to maintain pH at 7.4 at 37°C (Peart and Headrick, 2003; Reichelt *et al.*, 2009). Perfusion fluid was delivered at a coronary pressure of 80 mmHg, with coronary flow rate monitored via an ultrasonic flow probe proximal to the aortic cannula and left ventricular isovolumic function assessed via a fluid-filled balloon inflated to an initial end-diastolic pressure of 5 mmHg (Peart and Headrick, 2003; Reichelt *et al.*, 2009). Hearts were then stabilized for a period of 20 min.

No hearts met previously detailed exclusion criteria (Reichelt *et al.*, 2009).

After 20 min stabilization hearts were subjected to 25 min global normothermic ischemia and 45 min reperfusion. Coronary effluent was collected for analysis of LDH release, previously shown to correlate with infarction in this model (Peart and Headrick, 2003). Hearts were untreated (DMSO vehicle; *n*=6) or received 1 or 5 μM MDIVI-1 or 1 μM dynasore hydrate (*n*=8, 8 and 6, respectively), with infusion initiated 10-20 min prior to ischemia and maintained through reperfusion. These MDIVI-1 concentrations correspond to those reportedly protecting perfused hearts (Gao *et al*., 2013; Gharanei *et al.* 2013; Sharp *et al*. 2014), and are predicted to be selective for DRP-1 GTPase/fission inhibition (Cassidy-Stone *et al*., 2008; Numadate *et al*., 2014). The 1 μM dynasore concentration also mimics that mediating protection in prior heart studies (Gao *et al*., 2013), and is predicted to be selective for inhibition of dynamin/DRP-1 GTPase activities (Macia *et al*., 2006).

Mouse Heart Mitochondrial Respiratory Analyses

Mitochondrial O_2 consumption was quantified using an Oxygraph-2k instrument (Oroboros Instruments, Innsbruck, Austria) in shredded left ventricular myocardium from vehicle and 1 μM MDIVI-1 treated hearts sampled: prior to ischemia (*n*=4 and 6, respectively); at 10 min reperfusion (*n*=8 for both groups); or 45 min reperfusion (*n*=8 for both groups). Oxygraph chambers were cleaned before each analysis and stabilized with Mir05 media before addition of shredded myocardium (1 mg/mL in each chamber) and catalase (280 U/ml). Mitochondrial respiration via complexes I and complex II (at 37°C) was interrogated via sequential addition of complex-specific substrates and inhibitors: complex I substrates (5 mM pyruvate, 2 mM malate, 10 mM glutamate); complex II substrate (10 mM succinate); stimulation of oxidative phosphorylation (1 mM ADP); and mitochondrial un-coupling (0.5 μM FCCP).

H9c2 Myoblast Studies

To further explore the influences of MDIVI-1 on cardiac stress responses we examined effects of MDIVI-1 on viability, mitochondrial membrane potential, and expression of DRP-1, OPA-1 and signaling proteins in H9c2 cardiomyoblasts exposed to H_2O_2. The H9c2 cell line was obtained from the American Type Culture Collection (ATCC, USA). Cells were maintained in high glucose DMEM supplemented with 10% FBS, maintained under 95% O_2 and 5% CO_2 (37°C), and were passaged no more than 15 times. The H9c2 cells were grown to 70-80% confluence in 100 mm plates before exposure to 400 μM H_2O_2 for 60 min. Cells were untreated (DMSO vehicle) or treated with 50 μM MDIVI-1 40 min prior to H_2O_2 exposure. A sub-set of cells were sampled after only 5 min H_2O_2 for analysis of early ERK1/2 signaling. The 50 μM MDIVI-1 concentration replicates that widely reported as mediating cytoprotection in myocardial cell models (Ong *et al*., 2010; Yu *et al*., 2011; Dong *et al*., 2016; Gao *et al*., 2016).

For analysis of cell death/cytotoxicity, release of LDH into the medium (IU/ml) was assayed enzymatically according to manufacturer's directions (Sigma-Aldrich, St. Louis, MO, USA). Assessment of metabolic activity was undertaken via the colorimetric MTT (3-(4,5-dimethylthiazol-2-yl)-2,5-diphenyltetrazolium bromide) assay, according to manufacturer directions (Sigma-Aldrich, St. Louis, MO, USA), with reduction of the tetrazolium dye to colored formazan reflecting cellular NAD(P)H-dependent oxidoreductase activity.

H9c2 Mitochondrial Respiratory Analysis

For respiratory analysis, H9c2 cells were plated $1.0x10^4$ cells/well in 8-well XFp mini-plates in DMEM supplemented with 10% FBS and Penstrep, and left to attach overnight in an incubator (37°C 5% CO_2 / 95% O_2). Prior to analysis full media was replaced with XFp assay modified media (1 mM Pyruvate, 2 mM glutamine, 10 mM glucose, pH 7.4) and cells were

incubated in a 37°C non-CO_2 incubator for 45 min. Control and H_2O_2 (400 μM) challenged cells were pretreated with vehicle or 50 μM MDIVI-1 or 50 μM dynasore for 40 min. A Seahorse XFp Extracellular Flux Analyzer (Agilent Technologies Australia, Mulgrave VIC, Australia) was used to measure O_2 consumption rate (OCR) and extracellular acidification rate (ECAR). Measurements were performed over 6 min in measurement cycles of 4 (basal metabolic rate) or 3 (to assess metabolic rate under mitochondrial stress conditions). After basal OCR was established, oligomycin (1 μM), FCCP (2 μM; concentration based on titration experiments) and rotenone + antimycin A (0.5 μM) were injected sequentially (see **Fig. 11**), and mitochondrial parameters determined: basal respiration ($OCR_{Baseline}$ - $OCR_{Antimycin\ A+Rotenone}$), non-mitochondrial respiration ($OCR_{Rotenone+Antimycin\ A}$), ATP production ($OCR_{Baseline}$ - $OCR_{Oligomycin}$), proton leak ($OCR_{Oligomycin}$ - $OCR_{Rotenone+Antimycin\ A}$), peak respiration ($OCR_{FCCP}$ - $OCR_{Rotenone+Antimycin\ A}$), spare capacity ($OCR_{FCCP}$ – $OCR_{Baseline}$). All measurements were normalized to protein content per well. Data were analyzed by Seahorse Wave Software (Agilent, USA) using report generator.

Protein Analysis

*Tissue extraction***.** Post-ischemic protein expression was assessed in ventricular myocardium sampled at 45 min reperfusion (*n*=6, 8 and 6 for control, 1 μM MDIVI-1, and 1 μM dynasore groups, respectively). Tissue was sectioned and homogenized in a glass dounce with 1.0 mL of ice-cold isolation buffer containing protease and phosphatase inhibitors (70 mM sucrose, 190 mM mannitol, 20 mM HEPES and 0.2 mM EDTA, 1 mM PMSF, 10 μM leupeptin, 3 mM benzamidine, 5 μM pepstatin A, 1 mM NaO). Whole homogenate samples were removed and stored in lysis buffer for later analysis. Tissue homogenates underwent centrifugation at 600g (rcf) for 10 min at 4°C. The supernatant was removed and the nuclear pellet washed, spun at 600g for 10 min before re-suspension in lysis buffer and storage. The supernatant containing

mitochondria, cytosol and plasma membrane was centrifuged at 10,000g for 30 min, and the mitochondria enriched pellet re-suspended in lysis buffer

For H9c2 myoblasts, cells were harvested, washed with PBS and suspended in 150 μL of ice-cold lysis buffer (0.1% Triton-X; 20 mM MOPS, 2 mM EGTA, 5 mM EDTA, 30 mM sodium fluoride, 20 mM sodium tetra-pyrophosphate, 10 μM leupeptin, 5 μM pepstatin A, 3 mM benzamidine, 1 mM phenylmethanesulfonyl fluoride, 1 mM sodium orthovanadate). Cell lysates were frozen at -80°C until analysis. Thawed samples were prepared in required volumes with loading dye, and denatured at 95°C for 5 min in a heating block.

Protein concentrations were determined using a BCA assay in a 96-well microplate (Pierce BCA protein assay kit), with absorbance measured at 562 nm (Tecan infinite M200 Pro, Mannedorf, Switzerland). Aliquots of 20 μg protein were prepared with appropriate volumes of Kinexus buffer and protease inhibitors (20 mM MOPS, 2 mM EGTA; 5 mM EDTA; 30 mM sodium fluoride; 40 mM β-glycerophosphate; 20 mM sodium tetra-pyrophosphate) and stored at -80°C until analysis.

Electrophoresis. Myocardial or cell fractions containing equal quantities of protein were loaded onto hand-cast 10% acrylamide gels and separated in a Bio-Rad electrophoresis chamber at 150 V for 80 min. Transfer of proteins was achieved using a polyvinylidene difluoride fluorescence (PVDF) membrane at a 350 mA current for ~2 hrs, and blocked with Odyssey blocking buffer for a further 2 hrs at room temperature. Transferred proteins were incubated with primary antibody (dilution 1:750-1:1000) for 15-18 hrs at 4°C with gentle rocking. The PVDF membrane was washed in TBS for 5 min and again in TBST (4 cycles of 5 min) before incubation with secondary antibody at room temperature in the dark. Membranes were subsequently visualized on a Li-Cor Odyssey Infrared Imaging System (Li-Cor Biosciences, Lincoln, NE USA) with protein densitometry normalized to an internal standard and loading control.

Statistical Analyses

Data are expressed as means ± SEM. Differences between two or more groups were tested via 1- or 2-way ANOVA, with a Newman-Keuls post-hoc test applied when significant effects were detected. Significant differences were accepted for $P<0.05$. All tests were performed with Prism 6 (GraphPad Software Inc., La Jolla, CA).

Results

Mouse Heart Model - Effects Of DRP-1 Inhibitors On Baseline Function And Ischemic Contracture. Baseline contractile function and coronary flow were not significantly modified by either 1 or 5 μM MDIVI-1, or 1 μM dynasore (**Table 1**). As a gauge of potential benefit during ischemia itself we assessed rate and extent of ischemic contracture development. Onset of ischemic contracture, defined here as an increase of ≥20 mmHg above pre-ischemic pressure, occurred after ~270 sec in untreated hearts, with a peak pressure of 80 mmHg achieved at ~400 sec (**Fig. 2**). Treatment with 1 μM MDIVI-1 or dynasore failed to influence contracture whereas 5 μM MDIVI-1 was significantly protective (reducing both rate of and peak contracture).

Mouse Heart Model – Effects Of DRP-1 Inhibitors On I-R Injury. Left ventricular developed pressure (LVDP) gradually recovered to ~40% of pre-ischemic levels during 45 min reperfusion in untreated hearts (**Fig. 3**). Treatment with 1 μM MDIVI-1 significantly improved final recoveries of left ventricular diastolic, systolic and developed pressures (**Fig. 3**). Paradoxically, 5 μM MDIVI-1 appeared to modestly worsen recovery of contractile function, while 1 μM dynasore was without effect (**Fig. 3**).

Efflux of LDH was employed as a biomarker of cell death. We assessed total post-ischemic death, and in the case of 1 μM MDIVI-1 early damage over the initial 10 min of

reperfusion. Total post-ischemic LDH efflux was unaltered with 1 μM MDIVI-1 (**Fig. 4A**), however early LDH efflux to 10 min reperfusion was substantially reduced by >60% (**Fig. 4B**). A higher 5 μM MDIVI-1 concentration significantly reduced overall cell death. Conversely, LDH efflux was increased in hearts treated with 1 μM dynasore (**Fig. 4A**).

Mouse Heart Model – Effects Of DRP-1 Inhibitors On DRP-1 And Survival Kinases. Data indicate MDIVI-1 reduces mitochondrial DRP-1 expression without substantially influencing non-mitochondrial levels in post-ischemic myocardium (**Fig. 5**). In contrast, dynasore significantly reduced non-mitochondrial DRP-1 without influencing mitochondrial levels. The phosphorylation state of ERK1/2 at 10 min of reperfusion was significantly reduced in the non-mitochondrial fraction (**Fig. 6B,C**). Post-ischemic AKT expression and phosphorylation were unaltered by MDIVI-1 (**Fig. 6D-F**).

Mouse Heart Model – Effects Of DRP-1 Inhibitors On Post-Ischemic Respiratory Function. Substrate-dependent mitochondrial respiration was assessed in shredded myocardium from hearts subjected to normoxic perfusion, or 10 or 45 min post-ischemic reperfusion (± 1 μM MDIVI-1) (**Fig. 7**). Progressive reductions (up to 50%) in complex I activity, and the complex I flux control ratio, were evident during reperfusion (**Fig. 7**). Other respiratory parameters were relatively insensitive to I-R (**Fig. 7**). Treatment with MDIVI-1 did not significantly alter O_2 fluxes under normoxic or post-ischemic conditions. However, the post-ischemic decline in complex I flux control ratio was countered by MDIVI-1 (**Fig. 7**).

Rat H9c2 Model - Effects Of MDIVI-1 On Cytotoxicity, Metabolic Activity, Mitochondrial Membrane Potential And Morphology. Exposure of H9c2 cells to H_2O_2 for 60 min resulted in a 25% fall in metabolic activity (MTT assay) and significant cytotoxicity (100% increase in LDH release) (**Fig. 8**). Interestingly, treatment with 50 μM MDIVI-1 alone appeared to induce some cytotoxicity under baseline conditions, and failed to reduce

cytotoxicity during H_2O_2 challenge. However, MDIVI-1 significantly inhibited H_2O_2 dependent changes in metabolic activity. Fluorescent imaging of H9c2 cells (**Supplemental Fig. 1**) confirms substantial mitochondrial fragmentation with H_2O_2 that is inhibited by MDIVI-1 and dynasore. Curiously, imaging suggests some fragmentation in response to the inhibitors alone. Preliminary flow cytometric analysis of $\Delta\psi_m$ using a potentially high quenching 100 μM TMRM concentration suggests a 20% fall in membrane potential with H_2O_2, an effect reversed by MDIVI-1 (**Supplemental Fig. 2**), whereas flow cytometric analysis with non-quenching 20 nM TMRM suggests mitochondrial membrane potential may be slightly reduced with MDIVI-1/Dynasore treatment, with increased MitoTracker green MFI with MDIVI-1 treatment (**Supplemental Fig. 3**).

Rat H9c2 Model - Effects Of MDIVI-1 On Fission, Fusion, Autophagy, Apoptosis And Survival Kinase Signaling. Expression of DRP-1 was reduced by H_2O_2, an effect attenuated by MDIVI-1 (**Fig. 9A**). Conversely, the fusion protein OPA1 was increased with H_2O_2, an effect also countered by MDIVI-1 (**Fig. 9B**). Expression levels for LC3B-II and Parkin were increased with H_2O_2 stress, while the LCB3-II/1 ratio was not significantly altered (**Fig. 9C-E**). Treatment with MDIVI-1 countered the rise in LC3B-II and reduced the LCB3-II/1 ratio, while augmenting Parkin expression. Exposure to H_2O_2 induced pro-apoptotic changes, significantly increasing the BAX:BCL2 ratio and PARP cleavage (**Fig. 9F-H**). MDIVI-1 exaggerated the BAX:BCL2 response while countering PARP cleavage.

Exposure to H_2O_2 triggered phospho-activation of ERK1/2 and AKT, with total ERK1/2 unchanged while total AKT fell by ~50% (**Fig. 10**). Final phospho-activation of ERK1/2 and AKT was augmented by MDIVI-1, while early activation of ERK1/2 was reduced (**Fig. 10B**). Treatment with MDIVI-1 resulted in a small (~10%) fall in ERK1/2 expression during H_2O_2 challenge, and inhibited early ERK1/2 phospho-activation (5 min H_2O_2) while exaggerating late activation (**Fig. 10B**). Baseline AKT expression was moderately suppressed by MDIVI-1,

with expression during H_2O_2 unaltered by the inhibitor (**Fig. 10C**). Pronounced phospho-activation of AKT with H_2O_2 was exaggerated by MDIVI-1 (**Fig. 10D**).

Rat H9c2 Model - Effects Of MDIVI-1 and Dynasore On Mitochondrial Respiratory And Glycolytic Function. Mitochondrial stress analysis using the Seahorse XFp Extracellular Flux Analyzer demonstrates that H_2O_2 significantly reduces O_2 consumption (basal, maximal and spare consumption, and non-mitochondrial) and ATP production without influencing the proton leak (**Fig. 11**). Neither agent (at relatively high and potentially less specific concentrations of 50 μM) modified respiratory rates or proton leak in non-stressed cells, and both induced similar effects in H_2O_2 stressed cells: partially countering the effects of H_2O_2 on non-mitochondrial O_2 consumption; selectively increasing proton leak in H_2O_2 challenged cells; and eliminating the effects of H_2O_2 on basal respiration (**Fig. 11**).

The basal ECAR, a measure of glycolytic lactate production, was highest in MDIV-1 and lowest in H_2O_2 treated cells (**Fig. 11**). Oxidative stress limited glycolytic activity during mitochondrial uncoupling, paralleling effects on O_2 consumption. Both inhibitors partially countered the effects of H_2O_2 on basal ECAR and peak glycolytic capacity during uncoupling. The ratio of OCR:ECAR, reflecting preference for oxidative phosphorylation *vs.* glycolysis in coupled mitochondria, was relatively insensitive to both H_2O_2 stress and the DRP-1 inhibitors.

Discussion

Roles of DRP-1 in myocardial stress-resistance, and mechanisms by which inhibitors modify injury, remain unclear. Although reportedly protective in hearts (Ong *et al.*, 2010; Gao *et al*., 2013; Gharanei *et al*., 2014; Sharp *et al.*, 2014), DRP-1 inhibition can also increase post-ischemic death in cardiac (Dong *et al.*, 2016) and neuronal cells (Zhang *et al.*, 2013). Data here

support some benefit with MDIVI-1 but not dynasore during myocardial ischemia and early reperfusion, including preserved respiratory control and delayed or reduced necrotic death (**Table 2**). Studies in cardiomyoblasts also support partial metabolic and mitochondrial protection, although cell death was unaltered. Complex effects on survival kinase, autophagy and apoptosis signaling (summarized in **Table 2**) may underpin these mixed outcomes, while DRP-1 independent mechanisms cannot be excluded.

DRP-1 inhibition in cardioprotection. Although mitochondrial dynamism is not a feature of healthy myocardium (Song and Dorn, 2015), and despite evidence increased fission can be protective (Papanicolaou *et al.,* 2012), it is possible stressors may promote an excessive and injurious fission. Pre- and post-ischemic MDIVI-1 reportedly reduces cardiac injury, mitochondrial dysfunction and fission when applied at 5 (Sharp *et al*., 2014) or 50 μM (Ong *et al*., 2010). We found 1 μM MDIVI-1 limited post-ischemic dysfunction and delayed cell death, whereas 5 μM MDIVI-1 reduced necrotic death and ischemic contracture yet paradoxically worsened dysfunction (**Table 2**). A dissociation of functional and survival outcomes with DRP-1 inhibitors agrees with prior reports (Gharanei *et al.* 2013; Sharp *et al*. 2014). In cardiomyoblasts MDIVI-1 also improved metabolic and mitochondrial responses without altering survival. Curiously, oxidative stress in myoblasts induced changes predicted to favor fusion (reduced DRP-1 *vs.* increased OPA-1), with MDIVI-1 countering these changes.

Benefit with MDIVI-1 during ischemia and early reperfusion is consistent with preconditioning effects of the compound (Ong *et al.*, 2010; Sharp *et al.*, 2014; Dong *et al.*, 2016), and may reflect inhibition of the early fission shown to be rapidly induced during ischemia in other cell types (Kumar *et al.*, 2016). Subsequent perturbations of kinase, autophagy and death signaling during later reperfusion (**Table 2**) may induce additional effects, potentially exaggerating injury (Zhang *et al.*, 2013; Dong *et al.*, 2016). Contrasting MDIVI-1, dynasore worsened death in reperfused hearts without influencing dysfunction. Though speculative, this

may reflect other influences of dynasore, which interferes with dynamin-dependent endocytosis (Macia *et al*., 2006) and disrupts membrane cholesterol and lipid rafts (Preta *et al*., 2015).

These distinct and paradoxical effects of MDIVI-1 and dynasore in different models raise questions regarding selectivity's and mechanisms. While not directly addressing mechanisms here, both inhibitors promote mitochondrial elongation in stressed myoblasts (**Supplemental Fig. 1**), and MDIVI-1 reduced mitochondrial DRP-1 in post-ischemic myocardium, consistent with prior observations (Ong *et al*., 2010; Sharp *et al*., 2014; Dong *et al*., 2016). In contrast, dynasore modified non-mitochondrial DRP-1 in stressed hearts, suggesting differing specificities. Dynasore inhibits dynamin 1/2 GTPase activities with an IC_{50} of 12-15 μM, and exerts similar inhibitory effects on DRP-1 GTPase activity without influencing other related or unrelated GTPases (Macia *et al*., 2006). The 1 μM concentration applied in hearts is thus considered to be relatively selective for dynamin/DRP-1 inhibition. Higher concentrations are employed to inhibit endocytosis, which may participate in either cardiac injury (Khaidakov *et al.,* 2014; Yang *et al.*, 2016) or protection (Most *et al.*, 2003). Yang *et al.* (2016) found, for example, that 80 μM dynasore reduced internalisation of cardioprotective K_{ATP} channels and infarct development during myocardial I-R. The drug is nonetheless attributed with dynamin-independent effects, including inhibition of membrane ruffling, destabilisation of F-actin and disruption of lipid rafts (Preta *et al*., 2015). The latter rafts are particularly important to cardiac and mitochondrial stress-resistance (Fridolfsson *et al*., 2014; Schilling *et al*., 2015).

MDIVI-1 similarly inhibits dynamin dependent GTPase activity, with an IC_{50} of 1-10 μM in yeast (consistent with that for fission inhibition) (Cassidy-Stone *et al*., 2008), and a K_i of 15 μM for mammalian DRP-1 GTPase activity (Numadate *et al.* 2014). In contrast, while Bordt *et al*. (2017) confirmed similar potency of MDIVI-1 in yeast, they found negligible inhibitory effects on mammalian activity ($K_i \geq 1$ mM). There is also evidence MDIVI-1 may

inhibit cardiac K^+ currents with an IC_{50} of ~12 μM (So *et al*., 2012), and inhibit complex I respiration and ROS generation independently of DRP-1 at 10-50 μM concentrations (Bordt *et al*., 2017), though Zhang *et al*. (2016) found such effects (together with increased proton leak) are DRP-1 dependent. We find no evidence for modulation of complex I in pre- or post-ischemic hearts or unstressed cells, although MDIVI-1 preserved the complex I flux control ratio in reperfused hearts and both inhibitors augmented proton leak in stressed cells (**Fig. 11**). Manczak *et al.* (2019) more recently provide support for specific inhibition of DRP-1 and mitochondrial fragmentation with MDIVI-1, however they also confirm differential outcomes with differing MDIVI-1 concentrations: cytoprotection at 25 μM *vs.* worsened oxidative stress and ATP depletion with 75 μM. Smith and Gallo (2017) recently concluded that a weight of published evidence supports select activity of ≤25 μM MDIVI-1 toward DRP-1 and fission, although they highlight counter evidence and the importance of publishing negative results challenging this view. As discussed below, MDIVI-1 induces complex effects on multiple determinants of stress-resistance.

Mitochondrial function. Bi-directional relationships exist between mitochondrial respiration and dynamism. While excessive fission can be detrimental, moderately increased fission improves cardiac mitochondrial coupling and function (Papanicolaou *et al.,* 2012), and DRP-1 inhibition induces respiratory dysfunction (Benard *et al.*, 2007). Such dysfunction promotes mitochondrial fission (Benard *et al.*, 2007; Plecita-Hlavata *et al.*, 2008; Wang *et al.*, 2012; Toyama *et al.*, 2016) and inter-related autophagy (Chu *et al.*, 2013; Kagan *et al.*, 2016). However, Disatnik *et al.* (2013) report improved state 3 (equivalent to complex I) respiratory activity with the DRP-1 inhibitor P110 in post-ischemic myocardium, and Ding *et al.* (2017) report improved post-ischemic respiratory function in hearts of diabetic mice treated with MDIVI-1. Thus, whether DRP-1 inhibition improves mitochondrial function is equivocal, and may depend upon degree and type of stress. Here normoxic and post-ischemic respiratory fluxes

were not significantly modified by selective concentrations of MDIVI-1, although complex I flux control was protected, reflecting improved coupling and potentially limiting ROS generation (Jheng *et al.*, 2012; Sharp *et al.*, 2014; Wang *et al.*, 2014). Observations in rat cardiomyoblasts support both mitochondrial benefit and detriment, with MDIVI-1 preserving basal respiration during H_2O_2 stress while MDIVI-1 and dynasore both increased proton leak and non-mitochondrial O_2 consumption. The latter will reduce respiratory efficiency and promote ROS generation, consistent with effects of DRP-1 knockdown (Benard *et al.*, 2007), protection with increased fission (Papanicolaou *et al.,* 2012), and increased basal respiration and proton leak in DRP-1 and autophagy deficient nematodes (Luz *et al.,* 2015). Modulation of fission and autophagy proteins with MDIVI-1 (**Fig. 9**, **Table 2**) may thus contribute to mixed benefit and dysfunction in mitochondria.

Survival kinase signaling. Since regulatory loops also exist between DRP-1 and ERK1/2 and AKT, DRP-1 inhibitors may disrupt reperfusion injury salvage kinase (RISK) pathways that normally limit mitochondrial dysfunction, mPTP activity and cell death (Hausenloy and Yellon, 2007). Both kinases are linked to fission and DRP-1: ERK1/2 phosphorylates DRP-1 (Kashatus et al., 2015; Serasinghe et al., 2015) and promotes fission in myocytes (Yu *et al.*, 2011), neuronal cells (Gan *et al.*, 2014) and fibroblasts (Prieto *et al.*, 2016); DRP-1 in turn activates ERK1/2 (Lim *et al.*, 2015); and DRP-1 inhibitors reportedly impair myocardial ERK1/2 signaling while augmenting AKT signaling (Jheng *et al.*, 2012; Gharanei *et al.*, 2013). There is also some evidence for fusion protein involvement in protection via ERK1/2 (Pyakurel *et al.,* 2015) and PI3K/AKT (Ong *et al.,* 2015), although these outcomes may be fusion/fission independent (Ong *et al.,* 2017). Effects of MDIVI-1 here confirm linkages between DRP-1 and survival kinases, though effects are model specific: MDIVI-1 reduced post-ischemic ERK1/2 activation in hearts and early ERK1/2 activation in stressed myoblasts, while augmenting late ERK1/2 and AKT phosphorylation in myoblasts. These differential effects may be either

beneficial or detrimental - although ERK1/2 is implicated in the protective RISK pathway (Hausenloy and Yellon, 2007), and inhibition of early ERK1/2 activation may suppress early fission (Yu *et al.*, 2011), exaggeration of late ERK1/2 activation could worsen cell death (Koinzer *et al.*, 2015). On the other hand, increased AKT phosphorylation with MDIVI-1 is predicted to be protective, and may influence fusion proteins (Ong and Hausenloy, 2010; Ong *et al.,* 2015). Gharanei *et al.* (2013) report augmented myocardial AKT activation with MDIVI-1, inconsistent with insensitivity of cardiac AKT here (**Fig. 6**), though consistent with effects in myoblasts (**Fig. 9**). Disrupted kinase signaling may contribute to the mixed impacts of DRP-1 inhibition on stress responses. The basis of distinct effects in post-ischemic hearts *vs.* stressed myoblasts is unknown, though may involve differences in models, insults and concentrations of MDIVI-1 employed.

Autophagy proteins. Elevations in LC3B-II and Parkin in H_2O_2 treated myoblasts (**Fig. 9**) are consistent with stress-dependent induction of autophagy (Ha *et al.*, 2012). This process governs mitochondrial function (Gottlieb and Gustafsson, 2011; Dutta *et al.*, 2013), ischemic tolerance and cardioprotection (Moyzis *et al.*, 2015). Nonetheless, autophagy may also promote (Adhami *et al.*, 2006; Wen *et al.*, 2014) or inhibit I-R injury (Zhang *et al.*, 2013; Yun *et al.*, 2014). Moreover, while inhibition, deletion or mutation of DRP-1 inhibits autophagy (Arnoult *et al.*, 2005; Twig *et al.*, 2008; Dagda *et al.*, 2009), effects of DRP-1 *vs.* fission on this process and related cell death paths remain contentious within and across cell types. For example, fission may inhibit (Song *et al.*, 2015) or promote (Ikeda *et al.*, 2015) autophagy and death in cardiac cells, promote autophagy while inhibiting death in neuronal cells (Zhang *et al.*, 2013), and conversely inhibit autophagy while promoting death in renal cells (Lee *et al.*, 2016). The response of autophagy proteins to H_2O_2 was differentially modified by MDIVI-1: reductions in LC3B-II and the LC3B-II:I ratio suggest repressed autophagosome formation, consistent with reported effects of DRP-1 inhibition or knockdown (Twig *et al.*, 2008; Zhang *et al.*, 2013; Song

et al., 2015), and an observed decline in PARP (which normally promotes autophagy; **Fig. 9**). Conversely, observed Parkin up-regulation may favor autophagy, although elevated Parkin does not necessarily induce mitophagy (Morán *et al.*, 2014), and DRP-1 may be more important in Parkin *independent* autophagy (Kageyama *et al.*, 2014). There is also evidence Parkin can stimulate DRP-1 dependent fission (Yu *et al.*, 2011; Buhlman *et al.*, 2014), thus up-regulation may compensate in part for DRP-1 inhibition.

Cell death proteins. Since DRP-1 and fission also influence apoptosis, DRP-1 inhibitors are predicted to modulate apoptosis proteins. DRP-1 co-localizes with BAX (Karbowski *et al.*, 2002) and promotes BAX/BAK-induced cytochrome *c* release (Clerc *et al.*, 2014), and fragmentation during apoptosis is DRP-1 dependent (Frank *et al.*, 2001). Nonetheless, fission/DRP-1 may be dispensable in apoptotic death (Parone *et al.*, 2006; Ishihara *et al.*, 2009), and reportedly inhibit (Szabadkai *et al.*, 2004) and promote (Lee *et al.*, 2016) apoptosis in different cells. As for kinase signaling and autophagy, MDIVI-1 differentially modified cell death determinants, countering PARP cleavage and exaggerating BAX:BCL2 responses to H_2O_2 in cardiomyoblasts. How these changes influence death *vs.* survival is unclear - while increased BAX:BCL2 may promote apoptosis, reduced downstream PARP cleavage suggests a reduction in caspase activation. Inhibition of PARP cleavage has also been shown to induce necrosis (Herceg and Wang, 1999), with cleavage potentially serving as a switch between necrotic and apoptotic paths, while inhibiting necroptosis and parthanatos (Aredia and Scovassi, 2014). Suppression of cleavage by MDIVI-1 may thus exaggerate necrosis/necroptosis while limiting apoptosis, congruent with observations in stressed myocytes (Dong *et al.* 2016). Reduced cleavage may also favor autophagy and increase NAD consumption (Aredia and Scovassi, 2014), further influencing mitochondrial function and cell death. The effects of fission or DRP-1 on these processes warrant further study, as mixed impacts of MDIVI-1 may reflect opposing shifts in death pathways (Dong *et al.* 2016).

Evidence of a biphasic pattern of early ischemic fission followed by a post-ischemic wave preceding death (Kumar *et al.*, 2016) is relevant when considering effects of DRP-1 (Zhang *et al.*, 2013; Dong *et al.*, 2016). Early fission may be activated by rapid mitochondrial depolarization/inhibition (Benard *et al.*, 2007; Plecita-Hlavata *et al.*, 2008; Wang *et al.*, 2012; Toyama *et al.*, 2016) during ischemia, and could trigger cell death. However, whether this or the later post-ischemic wave of fission (Kumar *et al.*, 2016) facilitates apoptosis without playing essential roles (Parone *et al.*, 2006; Ishihara *et al.*, 2009) is also unclear. Interestingly, analysis of rotenone-dependent complex I inhibition (Benard *et al.*, 2007) supports a clear transition in mitochondrial morphology at the threshold to cell death that is consistent with fission.

Conclusions. The fission inhibitor MDIVI-1 reduces mitochondrial DRP-1 levels in post-ischemic myocardium, and improves mitochondrial control and function in both heart and cardiomyoblasts. Nonetheless, MDIVI-1 and dynasore produce complex outcomes in stressed hearts and cells, including differential changes in cell death *vs.* dysfunction, and survival-kinase, autophagy and cell death signaling. These observations raise important questions regarding the selectivity, mechanisms of action and broader cardioprotective utility of putative DRP-1 inhibitors.

Acknowledgements

Nil

Conflict of interest

The authors declare no conflicts of interest.

Author Contributions

Participated in research design: Wendt, Headrick, Peart, Du Toit

Conducted experiments: Wendt, See Hoe, Headrick, Vider

Performed data analysis: Wendt, Headrick, Vider, Peart

Wrote or contributed to writing of the manuscript: Wendt, Headrick, Peart, Du Toit

REFERENCES

Adhami F, Liao G, Morozov YM, Schloemer A, Schmithorst VJ, Lorenz JN, Dunn RS, Vorhees CV, Wills-Karp M, and Degen JL, et al. (2006) Cerebral ischemia-hypoxia induces intravascular coagulation and autophagy. *Am J Pathol* **169:** 566-583.

Aredia F and Scovassi AI (2014) Poly(ADP-ribose): a signaling molecule in different paradigms of cell death. Biochem Pharmacol **92**: 157-163.

Arnoult D, Rismanchi N, Grodet A, Roberts RG, Seeburg DP, Estaquier J, Sheng M, and Blackstone C (2005) Bax/Bak-dependent release of DDP/TIMM8a promotes Drp1- mediated mitochondrial fission and mitoptosis during programmed cell death. *Curr Biol* **15**: 2112-2118.

Benard G, Bellance N, James D, Parrone P, Fernandez H, Letellier T, and Rossignol R (2007) Mitochondrial bioenergetics and structural network organization. *J Cell Sci* **120**: 838- 848.

Biala AK, Dhingra R, and Kirshenbaum LA (2015) Mitochondrial dynamics: Orchestrating the journey to advanced age. *J Mol Cell Cardiol* **83**: 37-43.

Bordt EA, Clerc P, Roelofs BA, Saladino AJ, Tretter L, Adam-Vizi V, Cherok E, Khalil A, Yadava N, and Ge SX, et al. (2017) The Putative Drp1 inhibitor mdivi-1 Is a reversible mitochondrial complex i inhibitor that modulates reactive oxygen species. *Dev Cell* **40**: 583-594

Buhlman L, Damiano M, Bertolin G, Ferrando-Miguel R, Lombes A, Brice A, and Corti O (2014) Functional interplay between Parkin and Drp1 in mitochondrial fission and clearance. Biochim Biophys Acta **1843**: 2012-2026.

Cassidy-Stone A, Chipuk JE, Ingerman E, Song C, Yoo C, Kuwana T, Kurth MJ, Shaw JT, Hinshaw JE, and Green DR, et al. (2008) Chemical inhibition of the mitochondrial division dynamin reveals its role in Bax/Bak-dependent mitochondrial outer membrane permeabilization. *Dev Cell* **14**: 193-204.

Chen H and Chan DC (2005) Emerging functions of mammalian mitochondrial fusion and

fission. *Hum Mol Genet* **14**: R283-R289.

Chen H, Chomyn A, and Chan DC (2005) Disruption of fusion results in mitochondrial heterogeneity and dysfunction. J Biol Chem **280**: 26185-26192.

Chu CT, Ji J, Dagda RK, Jiang JF, Tyurina YY, Kapralov AA, Tyurin VA, Yanamala N, Shrivastava IH, and Mohammadyani D, et al. (2013) Cardiolipin externalization to the outer mitochondrial membrane acts as an elimination signal for mitophagy in neuronal cells. *Nat Cell Biol* **15**: 1197-1205.

Clerc P, Ge SX, Hwang H, Waddell J, Roelofs BA, Karbowski M, Sesaki H, and Polster BM (2014) Drp1 is dispensable for apoptotic cytochrome c release in primed MCF10A and fibroblast cells but affects Bcl-2 antagonist-induced respiratory changes. *Br J Pharmacol* **171**: 1988–1999.

Dagda RK, Cherra SJ, Kulich SM, Tandon A, Park D, and Chu CT (2009) Loss of PINK1 function promotes mitophagy through effects on oxidative stress and mitochondrial fission. *J Biol Chem* **284**: 13843-13855.

Disatnik MH, Ferreira JCB, Campos JC, Gomes KS, Dourado PMM, Qi X, and Mochly-Rosen D (2013) Acute inhibition of excessive mitochondrial fission after myocardial infarction prevents long-term cardiac dysfunction. *J Am Heart Assoc 2*: e000461.

Dong Y, Undyala VV, and Przyklenk K (2016) Inhibition of mitochondrial fission as a molecular target for cardioprotection: critical importance of the timing of treatment. *Basic Res Cardiol* **111**: 59.

Dorn GW 2nd (2015) Mitochondrial dynamism and heart disease: changing shape and shaping change. *EMBO Mol Med* **7**: 865-877.

Dorn GW 2nd, and Kitsis RN (2015) The mitochondrial dynamism-mitophagy-cell death interactome: multiple roles performed by members of a mitochondrial molecular ensemble. *Circ Res* **116**: 167-182.

Dutta D, Xu J, Kim JS, Dunn WA Jr, and Leeuwenburgh C (2013) Upregulated autophagy protects cardiomyocytes from oxidative stress-induced toxicity. *Autophagy* **9**: 328-344.

Frank S, Gaume B, Bergmann-Leitner ES, Leitner WW, Robert EG, Catez FDR, Smith CL, and Youle RJ (2001) The role of dynamin-related protein 1, a mediator of mitochondrial fission, in apoptosis. *Dev Cell* **1**: 515-525.

Fridolfsson HN, Roth DM, Insel PA, and Patel HH (2014) Regulation of intracellular signaling and function by caveolin. *FASEB J* **28**: 3823-3831.

Gan X, Huang S, Wu L, Wang Y, Hu G, Li G, Zhang H, Yu H, Swerdlow RH, Chen JX and Yan SS (2014) Inhibition of Erk-DLP1 signaling and mitochondrial division alleviates mitochondrial dysfunction in Alzheimer's disease cybrid cell. *Biochim Biophys Acta* **1842**: 220-231.

Gao D, Zhang L, Dhillon R, Hong TT, Shaw RM, and Zhu J (2013) Dynasore protects mitochondria and improves cardiac lusitropy in Langendorff perfused mouse heart. *PLoS One* **8**: e60967.

Gao D, Yang J, Wu Y, Wang Q, Wang Q, Lai EY, and Zhu J (2016) Targeting Dynamin 2 as a novel pathway to inhibit cardiomyocyte apoptosis following oxidative stress. *Cell Physiol Biochem* **39**: 2121-2134.

Gharanei M, Hussain A, Janneh O, and Maddock H (2013) Attenuation of doxorubicin- induced cardiotoxicity by mdivi-1: A mitochondrial division/mitophagy inhibitor. PLoS One **8**: e77713.

Gottlieb RA and Gustafsson AB (2011) Mitochondrial turnover in the heart. *Biochim Biophys Acta* **1813**: 1295-1301.

Ha JH, Noh HS, Shin IW, Hahm JR, and Kim DR (2012) Mitigation of H2O2-induced autophagic cell death by propofol in H9c2 cardiomyocytes. *Cell Biol Toxicol* **28**: 19-29.

Hausenloy DJ and Yellon DM (2007) Preconditioning and postconditioning: United at reperfusion. *Pharmacol Ther* **116**: 173-191.

Herceg Z and Wang ZQ (1999) Failure of poly(ADP-ribose) polymerase cleavage by caspases leads to induction of necrosis and enhanced apoptosis. *Mol Cell Biol* **19**: 5124–5133.

Ikeda Y, Shirakabe A, Maejima Y, Zhai P, Sciarretta S, Toli J, Nomura M, Mihara K, Egashira K, and Ohishi M, et al. (2015) Endogenous Drp1 mediates mitochondrial autophagy and protects the heart against energy stress. Circ Res **116**: 264-278.

Ishihara N, Nomura M, Jofuku A, Kato H, Suzuki SO, Masuda K, Otera H, Nakanishi Y, Nonaka I, and Goto Y, et al. (2009) Mitochondrial fission factor Drp1 is essential for embryonic development and synapse formation in mice. *Nat Cell Biol* **11**: 958-966.

Jheng HF, Tsai PH, Guo SM, Kuo LH, Chang CC, Su IJ, Chang CR, and Tsai YS (2012) Mitochondrial fission contributes to mitochondrial dysfunction and insulin resistance in skeletal muscle. *Mol Cell Biol* **32:** 309-319.

Kagan VE, Jiang J, Huang Z, Tyurina YY, Desbourdes C, Cottet-Rousselle C, Dar HH, Verma M, Tyurin VA, Kapralov AA, et al. (2016) NDPK-D (NM23-H4)-mediated externalization of cardiolipin enables elimination of depolarized mitochondria by mitophagy. *Cell Death Differ* **23**: 1140-1151.

Kageyama Y, Hoshijima M, Seo K, Bedja D, Sysa-Shah P, Andrabi SA, Chen W, Höke A, Dawson VL, and Dawson TM, et al. (2014) Parkin-independent mitophagy requires Drp1 and maintains the integrity of mammalian heart and brain. *EMBO J* **33**: 2798-2813.

Karbowski M, Lee YJ, Gaume B, Jeong SY, Frank S, Nechushtan A, Santel A, Fuller M, Smith C,L and Youle RJ (2002) Spatial and temporal association of Bax with mitochondrial fission sites, Drp1, and Mfn2 during apoptosis. *J Cell Biol* **159**: 931-938.

Kashatus JA, Nascimento A, Myers LJ, Sher A, Byrne FL, Hoehn KL, Counter CM, and Kashatus DF (2015) Erk2 phosphorylation of Drp1 promotes mitochondrial fission and MAPK-driven tumor growth. *Mol Cell* **57**: 537-551.

Khaidakov M, Mercanti F, Wang X, Ding Z, Dai Y, Romeo F, Sawamura T, and Mehta JL

(2014) Prevention of export of anoxia/reoxygenation injury from ischemic to nonischemic cardiomyocytes via inhibition of endocytosis. *Am J Physiol Heart Circ Physiol* **306**: H1700-H1707.

Koinzer S, Reinecke K, Herdegen T, Roider JK, and Lettner A (2015) Oxidative stress induces biphasic ERK1/2 activation in the RPE with distinct effects on cell survival at early and late activation. *Curr Eye Res* **40**: 853-857.

Kumar R, Bukowski MJ, Wider JM, Reynolds CA, Calo ., Lepore B, Tousignant R, Jones M, Przyklenk K, and Sanderson TH (2016) Mitochondrial dynamics following global cerebral ischemia. *Mol Cell Neurosci* **76**: 68-75.

Lee WC, Chiu CH, Chen JB, Chen CH, and Chang HW (2016) Mitochondrial fission increases apoptosis and decreases autophagy in renal proximal tubular epithelial cells treated with high glucose. *DNA Cell Biol* **35**: 657-665.

Lim S, Lee SY, Seo HH, Ham O, Lee C, Park JH, Lee J, Seung M, Yun I, Han SM, Lee S, Choi E, and Hwang KC (2015) Regulation of mitochondrial morphology by positive feedback interaction between PKC delta and Drp1 in vascular smooth muscle cell. *J Cell Biochem* **116**: 648-660.

Luz AL, Rooney JP, Kubik LL, Gonzalez CP, Song DH, and Meyer JN (2015) Mitochondrial morphology and fundamental parameters of the mitochondrial respiratory chain are altered in Caenorhabditis elegans strains deficient in mitochondrial dynamics and homeostasis processes. *PLoS One* **10**: e0130940.

Macia E, Ehrlich M, Massol R, Boucrot E, Brunner C, and Kirchhausen T (2006) Dynasore, a cell-permeable inhibitor of dynamin. *Dev Cell* **10**: 839-850.

Manczak M, Kandimalla R, Yin X, and Reddy PH (2019) Mitochondrial division inhibitor 1 reduces dynamin-related protein 1 and mitochondrial fission activity. *Hum Mol Genet* **28**: 177-199.

Marín-García J and Akhmedov AT (2016) Mitochondrial dynamics and cell death in heart failure. *Heart Fail Rev* **21**: 123-136.

Morán M, Delmiro A, Blázquez A, Ugalde C, Arenas J, and Martín MA (2014) Bulk autophagy, but not mitophagy, is increased in cellular model of mitochondrial disease. *Biochim Biophys Acta* **1842**: 1059-1070.

Most P, Boerries M, Eicher C, Schweda C, Ehlermann P, Pleger ST, Loeffler E, Koch WJ, Katus HA, and Schoenenberger CA et al (2003) Extracellular S100A1 protein inhibits apoptosis in ventricular cardiomyocytes via activation of the extracellular signal-regulated protein kinase 1/2 (ERK1/2). *J Biol Chem* **278**: 48404-48412.

Moyzis AG, Sadoshima J, and Gustafsson AB (2015) Mending a broken heart: the role of mitophagy in cardioprotection. *Am J Physiol Heart Circ Physiol* **308**: H183-H192.

Numadate A, Mita Y, Matsumoto Y, Fujii S, and Hashimoto Y (2014) Development of 2-thioxoquinazoline-4-one derivatives as dual and selective inhibitors of dynamin-related protein 1 (Drp1) and puromycin-sensitive aminopeptidase (PSA). *Chem Pharm Bull* (Tokyo) **62**: 979-988.

Ong SB and Hausenloy DJ (2010) Mitochondrial morphology and cardiovascular disease. *Cardiovasc Res* **88**: 16-29.

Ong SB, Subrayan S, Lim SY, Yellon DM, Davidson SM, and Hausenloy DJ (2010) Inhibiting mitochondrial fission protects the heart against ischemia/reperfusion injury. *Circulation* **121**: 2012-2022.

Ong SB, Hall AR, Dongworth RK, Kalkhoran S, Pyakurel A, Scorrano L, and Hausenloy DJ (2015) Akt protects the heart against ischaemia-reperfusion injury by modulating mitochondrial morphology. *Thromb Haemost* **113**: 513-521.

Ong, SB, Kalkhoran SB, Hernández-Reséndiz S, Samangouei P, Ong SG, and Hausenloy DJ (2017) Mitochondrial-shaping proteins in cardiac health and disease - the long and the short of

it! *Cardiovasc Drugs Ther* **31**: 87-107.

Papanicolaou KN, Ngoh GA, Dabkowski ER, O'Connell KA, Ribeiro RF Jr, Stanley WC, and Walsh K (2012) Cardiomyocyte deletion of mitofusin-1 leads to mitochondrial fragmentation and improves tolerance to ROS-induced mitochondrial dysfunction and cell death. *Am J Physiol Heart Circ Physiol* **302**: H167-H179.

Parone PA, James DI, Da Cruz S, Mattenberger Y, Donze O, Barja F, and Martinou JC (2006) Inhibiting the mitochondrial fission machinery does not prevent Bax/Bak-dependent apoptosis. *Mol Cell Biol* **26**: 7397-7408.

Peart J and Headrick JP (2003) Adenosine-mediated early preconditioning in mouse: protective signaling and concentration dependent effects. *Cardiovasc Res* **58**: 589-601. Plecita-Hlavata L, Lessard M, Santorova J, Bewersdorf J, and Jezek P (2008) Mitochondrial oxidative phosphorylation and energetic status are reflected by morphology of mitochondrial network in INS-1E and HEP-G2 cells viewed by 4Pi microscopy. *Biochim Biophys Acta* **1777**: 834-846.

Preta G, Cronin JG, and Sheldon IM (2015) Dynasore - not just a dynamin inhibitor. *Cell Commun Signal* **13**: 24.

Prieto J, Leon M, Ponsoda X, Sendra R, Bort R, Ferrer-Lorente R, Raya A, López- García C, and Torres J (2016) Early Erk1/2 activation promotes Drp1-dependent mitochondrial fission necessary for cell reprogramming. *Nat Commun* **7**: 11124.

Pyakurel A, Savoia C, Hess D, and Scorrano L (2015) Extracellular regulated kinase phosphorylates mitofusin 1 to control mitochondrial morphology and apoptosis. *Mol Cell* **58**: 244-254.

Reddy PH (2014) Inhibitors of mitochondrial fission as a therapeutic strategy for diseases with oxidative stress and mitochondrial dysfunction. *J Alzheimers Dis* **40**: 245-256.

Reichelt ME, Willems L, Hack BA, Peart JN, and Headrick JP (2009) Cardiac and coronary function in the Langendorff-perfused mouse heart model. *Exp Physiol* **94**: 54-70.

Rosdah AA, K Holien J, Delbridge LM, Dusting GJ, and Lim SY (2016) Mitochondrial fission - a drug target for cytoprotection or cytodestruction? *Pharmacol Res Perspect* **4**: e00235.

Schilling JM, Roth DM, and Patel HH (2015) Caveolins in cardioprotection – translatability and mechanisms. *Br J Pharmacol* **172**: 2114-2125.

Serasinghe MN, Wieder SY, Renault TT, Elkholi R, Asciolla JJ, Yao JL, Jabado O, Hoehn K, Kageyama Y, Sesaki H, et al. (2015) Mitochondrial division is requisite to RAS-induced transformation and targeted by oncogenic MAPK pathway inhibitors. *Mol Cell* **57**: 521-536.

Sharp WW, Fang YH, Han M, Zhang HJ, Hong Z, Banathy A, Morrow E, Ryan JJ, and Archer SL (2014) Dynamin-related protein 1 (Drp1)-mediated diastolic dysfunction in myocardial ischemia-reperfusion injury: therapeutic benefits of Drp1 inhibition to reduce mitochondrial fission. *FASEB J* **28**: 316-326.

Smith G and Gallo G (2017) To mdivi-1 or not to mdivi-1: Is that the question? *Dev Neurobiol* **77**: 1260-1268.

So EC, Hsing CH, Liang CH, and Wu SN (2012) The actions of mdivi-1, an inhibitor of mitochondrial fission, on rapidly activating delayed-rectifier K^+ current and membrane potential in HL-1 murine atrial cardiomyocytes. *Eur J Pharmacol* **683**: 1-9.

Song M and Dorn GW 2nd (2015) Mitoconfusion: noncanonical functioning of dynamism factors in static mitochondria of the heart. *Cell Metab* **21**: 195-205.

Song M, Mihara K, Chen Y, Scorrano L, and Dorn GW (2015) Mitochondrial fission and fusion factors reciprocally orchestrate mitophagic culling in mouse hearts and cultured fibroblasts. *Cell Metab* **21**: 273-285.

Szabadkai G, Simoni AM, Chami M, Wieckowski MR, Youle RJ, and Rizzuto R (2004) Drp-1-dependent division of the mitochondrial network blocks intraorganellar Ca^{2+} waves and protects against Ca^{2+} mediated apoptosis. *Mol Cell* **16**: 59-68.

Taguchi N, Ishihara N, Jofuku A, Oka T, and Mihara K (2007) Mitotic phosphorylation of

dynamin-related GTPase Drp1 participates in mitochondrial fission.*J Biol Chem* **282**:11521-9.

Toyama EQ, Herzig S, Courchet J, Lewis TL Jr, Loson OC, Hellberg K, Young NP, Chen H, Polleux F, Chan DC, and Shaw RJ (2016) Metabolism. AMP-activated protein kinase mediates mitochondrial fission in response to energy stress. *Science* **351**: 275- 281.

Twig G, Elorza A, Molina AJA, Mohamed H, Wikstrom JD, Walzer G, Stiles L, Haigh SE, Katz S, Las G, et al (2008) Fission and selective fusion govern mitochondrial segregation and elimination by autophagy. *EMBO J* **27**: 433-446.

Wang J, Wang P, Li S, Wang S, Li Y, Liang N, and Wang M (2014) Mdivi-1 prevents apoptosis induced by ischemia-reperfusion injury in primary hippocampal cells via inhibition of reactive oxygen species-activated mitochondrial pathway. *J Stroke Cerebrovasc Dis* **23**: 1491-1499.

Wang S, Xiao W, Shan S, Jiang C, Chen M, Zhang Y, Lü S, Chen J, Zhang C, Chen Q, and Long M (2012) Multi-patterned dynamics of mitochondrial fission and fusion in a living cell. *PLoS One* **7**: e19879.

Wen YD, Sheng R, Zhang LS, Han R, Zhang X, Zhang XD, Han F, Fukunaga K, and Qin ZH (2014) Neuronal injury in rat model of permanent focal cerebral ischemia is associated with activation of autophagic and lysosomal pathways. *Autophagy* **4**: 762-769.

Yang HQ, Foster MN, Jana K, Ho J, Rindler MJ, and Coetzee WA (2016) Plasticity of sarcolemmal K_{ATP} channel surface expression: relevance during ischemia and ischemic preconditioning. *Am J Physiol Heart Circ Physiol* **310**: H1558-H1566.

Yu T, Jhun BS, and Yoon Y (2011) High-glucose stimulation increases reactive oxygen species production through the calcium and mitogen-activated protein kinase-mediated activation of mitochondrial fission. *Antioxid Redox Signal* **14**: 425-437.

Yu W, Sun Y, Guo S, and Lu B (2011) The PINK1/Parkin pathway regulates mitochondrial dynamics and function in mammalian hippocampal and dopaminergic neurons. *Hum Mol Genet* **20**: 3227-3240.

Yun N, Cho HI, and Lee SM (2014) Impaired autophagy contributes to hepatocellular damage during ischemia/reperfusion: Heme oxygenase-1 as a possible regulator. *Free Radic Biol Med* **68**: 168-177.

Zhang X, Yan H, Yuan Y, Gao J, Shen Z, Cheng Y, Shen Y, Wang RR, Wang X, Hu WW, Wang G, and Chen Z (2013) Cerebral ischemia-reperfusion-induced autophagy protects against neuronal injury by mitochondrial clearance. *Autophagy* **9**: 1321-1333.

Zhang H, Wang P, Bisetto S, Yoon Y, Chen Q, Sheu SS, and Wang W (2017) A novel fission-independent role of dynamin-related protein 1 in cardiac mitochondrial respiration. *Cardiovasc Res* **113**: 160-170.

FOOTNOTES

*** Financial Support:**

L.W. was supported by a postgraduate scholarship from Griffith University, and L.E.S.H. was supported by a postgraduate scholarship from the National Heart Foundation of Australia. This research was supported by internal funds from Griffith University.

Previous presentations of work at meetings

Effects of Dynamin-Related Protein-1 (DRP-1) Inhibition with MDIVI-1 on Myocardial Injury, Mitochondrial Respiration and Stress-Signalling in the Murine Heart. 2015. Wendt L, See Hoe L, Sachaphibulkij K, Du toit E, Peart J, Headrick J. *The FASEB Journal* **29**: 1_suppment, supplement 1026.2

Reprint requests contact:

Prof. John P. Headrick

School of Medical Science

Griffith University

Southport QLD 4217

AUSTRALIA

E-mail: J.Headrick@griffith.edu.au

LEGENDS FOR FIGURES

Fig. 1. Chemical structures of the putative DRP-1 inhibitors MDIVI-1 (PubChem CID: 3825829) and dynasore (PubChem CID: 136239889).

Fig. 2. Impacts of MDIVI-1 and dynasore on myocardial ischemic contracture. Hearts were untreated (CTRL) or pre-treated with 1 μM dynasore (DYN) or 1-5 μM MDIVI-1 10 min prior to and throughout I-R. **A)** Time to ischemic contracture; **B)** time to peak ischemic contracture**; C)** peak ischemic contracture. Data are means ± SEM (*n*=6-8/group). *, P<0.05 *vs*. CTRL; by 1-way ANOVA and Newman-Keuls post-hoc test.

Fig. 3. Effects of MDIVI-1 and dynasore on myocardial dysfunction post-ischemia. Post-ischemic functional recoveries are shown for untreated (CTRL) hearts, and hearts treated with 1 μM dynasore (DYN) or 1-5 μM MDIVI-1 10 min prior to and throughout I-R. **A)** Patterns of recovery for left ventricular developed pressure (LVDP); and final recoveries for **B)** end-diastolic, **C)** systolic; and **D)** developed pressures. Data are means ± SEM (*n*=6-8/group). *, P<0.05 *vs*. untreated (CTRL); †, P<0.05 5 *vs*. 1 μM MDIVI-1; by 2-way ANOVA (**A**) and 1-way ANOVA (**B, C**) and Newman-Keuls post-hoc test.

Fig. 4. Effects of DRP-1 inhibitors on post-ischemic LDH efflux. A) Total lactate dehydrogenase (LDH) efflux throughout 25 min ischemia/45 min reperfusion in untreated hearts (CTRL), and hearts treated with 1 μM dynasore (DYN) or 1-5 μM MDIVI-1 10 min prior to and throughout I-R. **B)** Early LDH release over initial 10 min reperfusion in hearts untreated or treated with 1 μM MDIVI-1. Efflux is shown in international units (IU). Means ± SEM (*n*=6-8/group). *, P<0.05 *vs*. untreated (CTRL) or Baseline; †, P<0.05 5 *vs*. 1 μM MDIVI-

1; by 1-way ANOVA and Newman-Keuls post-hoc test.

Fig. 5. Effects of DRP-1 inhibitors on post-ischemic DRP-1 expression. Relative expression of DRP-1 in **A)** mitochondrial, and **B)** non-mitochondrial fractions from hearts subjected to 25 min ischemia and 45 min reperfusion. Perfused hearts were untreated (CTRL), or treated with 1 μM dynasore (DYN) or MDIVI-1 10 min prior to and throughout I-R. Data are means ± SEM (*n*=6-8/group). *, P<0.05 *vs.* untreated (CTRL); †, *P*<0.05 *vs*. dynasore (DYN); by 1-way ANOVA and Newman-Keuls post-hoc test.

Fig. 6. Effects of MDIVI-1 on post-ischemic ERK1/2 and AKT expression and phosphorylation. Mitochondrial and non-mitochondrial fractions from hearts reperfused for 10 min following 25 min ischemia were assessed for: **A)** total ERK1/2; **B)** phosphorylated ERK1/2; **C)** the ratio of phosphorylated:total ERK1/2; **D)** total AKT; **E)** phosphorylated AKT; and **F)** the ratio of phosphorylated:total AKT. Hearts were untreated (CTRL) or treated with 1 μM MDIVI-1 10 min prior to and throughout I-R. Lower panel; presents immunoblot images for total and phosphoproteins in mitochondrial and non-mitochondrial fractions. Mitochondrial expression normalized to COX-IV; non-mitochondrial expression to GAPDH. Data are means ± SEM (*n*=4-8/group). *, P<0.05 *vs.* untreated (CTRL); †, P<0.05 mitochondrial *vs.* cytosolic phospho:total ratio; by 1-way ANOVA and Newman-Keuls post-hoc test.

Fig. 7. Effects of I-R and MDIVI-1 on mitochondrial respiration. Hearts were perfused under normoxic conditions, or reperfused for 10 or 45 min following 25 min ischemia. Perfused hearts were untreated (CTRL) or exposed to 1 μM MDIVI-1 10 min prior to and throughout I-R. Data are shown for: Complex I leak state (addition of 5 mM pyruvate/2 mM malate/10 mM glutamate); Complex I oxidative phosphorylation (OxPhos) capacity (addition of 5 mM ADP);

Complex I respiratory flux (ETS capacity - Leak); Complex I flux control ratio (normalized to uncoupled respiration upon addition of FCCP); Complex I + Complex II OxPhos capacity (10 mM succinate/5 mM ADP); and Complex I + Complex II electron transfer system (ETS) capacity (addition of 0.5 μM FCCP). Oxygen flux values are normalized to mg ventricular tissue per chamber. Data are means ± SEM (*n*=4-8/group). *, P<0.05 *vs*. Normoxia; †, P<0.05 *vs*. untreated (CTRL); by 1- way ANOVA and Newman-Keuls post-hoc test.

Fig. 8. Effects of MDIVI-1 on metabolic activity and cell death in H9c2 cardiomyoblasts exposed to H_2O_2. Cells were pre-treated with vehicle (CTRL) or 50 μM MDIVI-1 prior to 60 min H_2O_2 exposure (400 μM). Data are shown for: **A)** cellular metabolic activity (MTT assay, relative to baseline); and **B)** cell death (total LDH efflux). Data are means ± SEM (*n*=3). *, P<0.05 *vs*. Baseline; †, P<0.05 *vs*. untreated (CTRL); by 1-way ANOVA and Newman-Keuls post-hoc test.

Fig. 9. Effects of MDIVI-1 on fission/fusion, autophagy and apoptosis proteins in H9c2 cardiomyoblasts exposed to H_2O_2. Cells were pre-treated with vehicle (CTRL) or 50 μM MDIVI-1 prior to 60 min H_2O_2 exposure (400 μM). Cell lysates were assessed for: DRP-1; OPA-1; ratio of LC3B-II:LC3B-I; Parkin; ratio of BAX:BCL2; and PARP cleavage. Protein levels are normalized to GAPDH expression. Immunoblot images shown at the top of each panel. Data are means ± SEM (*n*=3). *, P<0.05 *vs*. Baseline; †, P<0.05 *vs*. untreated (CTRL); by 1-way ANOVA and Newman-Keuls post-hoc test.

Fig. 10. Effects of MDIVI-1 on survival kinase signaling in H9c2 cardiomyoblasts exposed to H_2O_2. Cells were pre-treated with vehicle or 50 μM MDIVI-1 prior to 60 min exposure to 400 μM H_2O_2. Cell lysates were assessed for: **A)** total ERK1/2; **B)** ratio of

phosphorylated: total (P:T) ERK1/2; **C)** total AKT; and **D)** ratio of phosphorylated:total (P:T) AKT. A sub-set were assessed for changes in early activation of ERK1/2 after 5 min H_2O_2 challenge. Right panel shows immunoblots for ERK1/2 (5 and 60 min H_2O_2) and AKT (60 min H_2O_2). Expression normalized to GAPDH. Data are means±SEM (*n*=5/group). *, P<0.05 *vs*. Baseline; †, P<0.05 *vs*. untreated (CTRL); by 1-way ANOVA and Newman-Keuls test.

Fig. 11. Effects of MDIVI-1 and dynasore on mitochondrial respiratory function and cellular acidification in H9c2 cardiomyoblasts exposed to H_2O_2. Cells were pre-treated with vehicle, 50 μM MDIVI-1 or dynasore prior to control conditions or exposure to 400 μM H_2O_2. ***Left Panels)*** Oxygen consumption rate (OCR) and extracellular acidification rate (ECAR, indicator of glycolytic metabolism) were monitored. ***Right Panels)*** The OCR data (pmol/min/ μg protein per well) were used to calculate respiratory parameters as indicated in **Materials and Methods**. Data are means ± SEM (*n*=3-5/group). *, P<0.05 *vs*. Control (Ctrl); †, P<0.05 *vs*. H_2O_2; by 1-way ANOVA and Newman-Keuls post-hoc test.

JPET Fast Forward. Published on November 8, 2019 as DOI: 10.1124/jpet.119.258897
This article has not been copyedited and formatted. The final version may differ from this version.

TABLES

TABLE 1

Function in *ex vivo* hearts prior to and after infusion of DRP-1 inhibitors

Treatment	Pre/Post Infusion	End-Diastolic Pressure (mmHg)	Systolic Pressure (mmHg)	Developed Pressure (mmHg)	Coronary Flow (ml/min)
Vehicle (*n*=6)	*Pre* - *Post* -	5 ± 1 5 ± 1	134 ± 3 132 ± 4	128 ± 6 126 ± 6	3.1 ± 0.2 3.4 ± 0.3
1 µM Dynasore (*n*=6)	*Pre* - *Post* -	4 ± 1 4 ± 1	135 ± 6 133 ± 7	131 ± 6 129 ± 7	2.9 ± 0.2 3.4 ± 0.2
1 µM MDIVI-1 (*n*=8)	*Pre* - *Post* -	5 ± 1 6 ± 1	122 ± 6 120 ± 6	117 ± 6 114 ± 7	2.6 ± 0.2 3.2 ± 0.2
5 µM MDIVI-1 (*n*=8)	*Pre* - *Post* -	7 ± 1 6 ± 1	144 ± 8 137 ± 8	124 ± 9 120 ± 10	2.7 ± 0.2 2.9 ± 0.2

Functional measures were made prior to and after 10 min of drug (or vehicle) infusion. Data are means ± SEM. No significant differences were detected pre- vs. post-treatment.

TABLE 2

Summary of MDIVI-1 effects in mouse hearts subjected to I-R and rat cardiomyoblasts exposed to H_2O_2.

Parameter/Protein	**Myocardial I-R**	**Myoblast Oxidative Stress**
Contractile or Metabolic Function	⇓ Contracture (5 μM) ⇑ LVP (1 μM); ⇓ LVP (5 μM)	⇑ MTT
Necrosis (LDH efflux)	Delayed (1 μM) ⇓ (5 μM)	⇔
Mitochondrial Function	⇑ CI Flux Control	⇑ $\Delta\psi_m$, ⇑ Basal OCR, ⇑ Non-Mito OCR, ⇑ Proton Leak
Fission/Fusion	⇓ DRP-1	⇓DRP-1, ⇑ OPA-1
Survival Kinases	⇓ P-ERK	⇑ P-AKT, ⇑ late P-ERK, ⇓ early P-ERK
Autophagy	-	⇑ Parkin, ⇓ LC3B-II, ⇓ LC3B-II/I
Apoptosis	-	⇓ PARP Cleavage, ⇑ BAX:BCL2

JPET Fast Forward. Published on November 8, 2019 as DOI: 10.1124/jpet.119.258897
This article has not been copyedited and formatted. The final version may differ from this version.

FIGURES

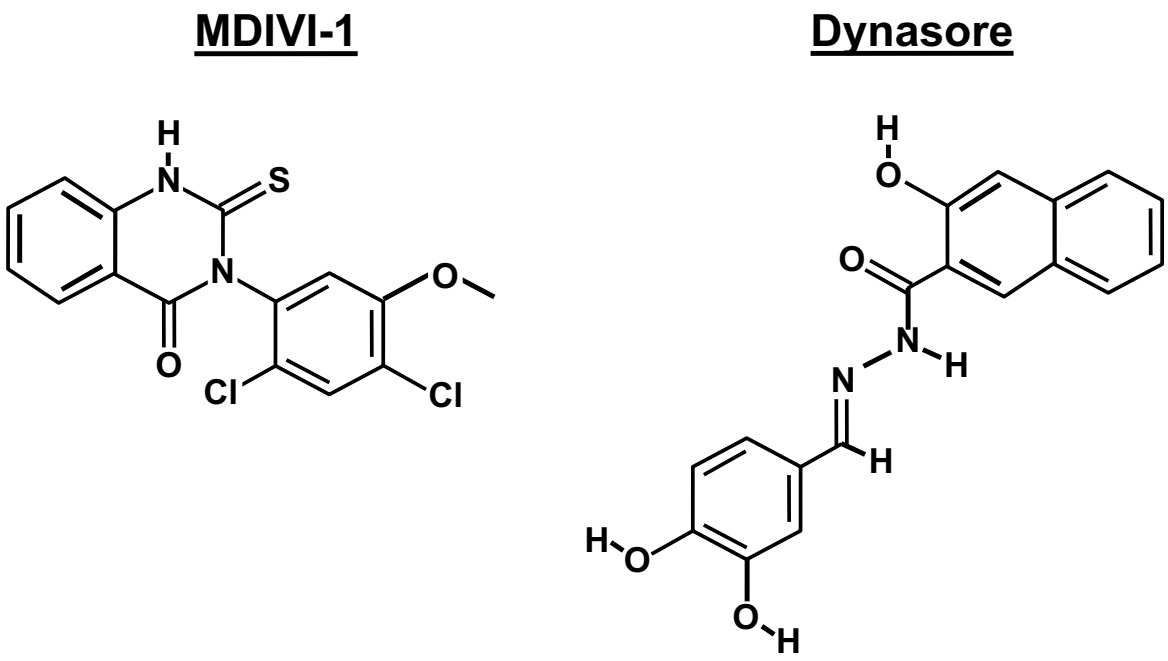

Fig. 1.

JPET Fast Forward. Published on November 8, 2019 as DOI: 10.1124/jpet.119.258897
This article has not been copyedited and formatted. The final version may differ from this version.

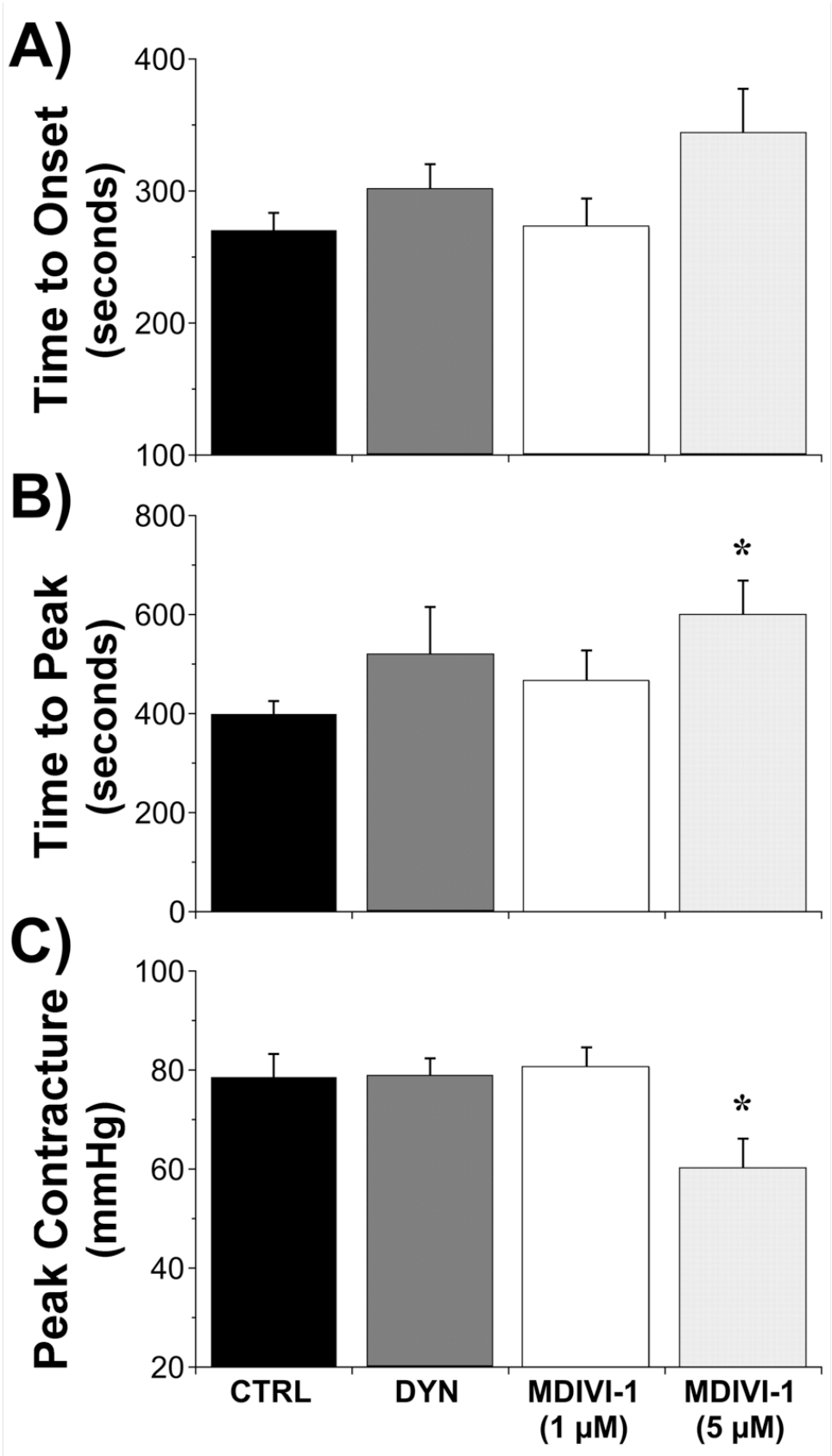

Fig. 2.

JPET Fast Forward. Published on November 8, 2019 as DOI: 10.1124/jpet.119.258897
This article has not been copyedited and formatted. The final version may differ from this version.

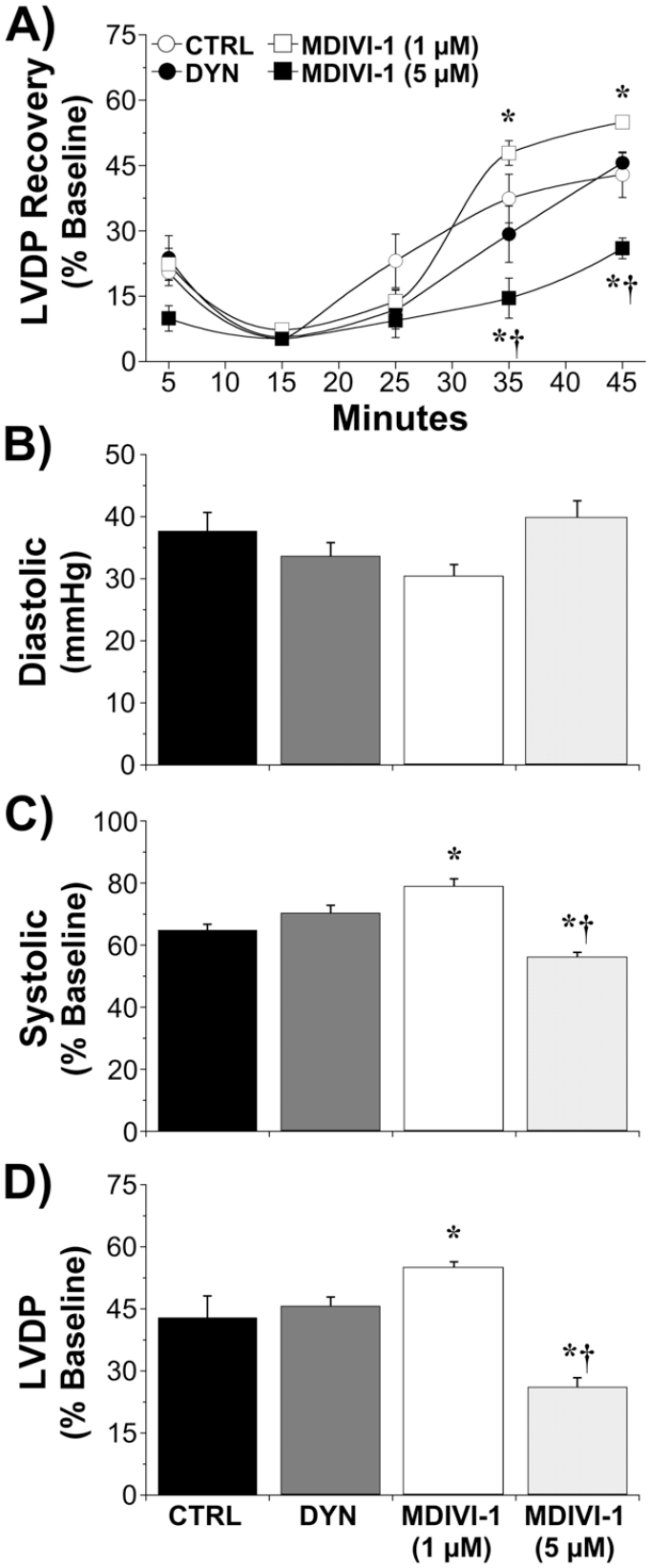

Fig. 3.

JPET Fast Forward. Published on November 8, 2019 as DOI: 10.1124/jpet.119.258897
This article has not been copyedited and formatted. The final version may differ from this version.

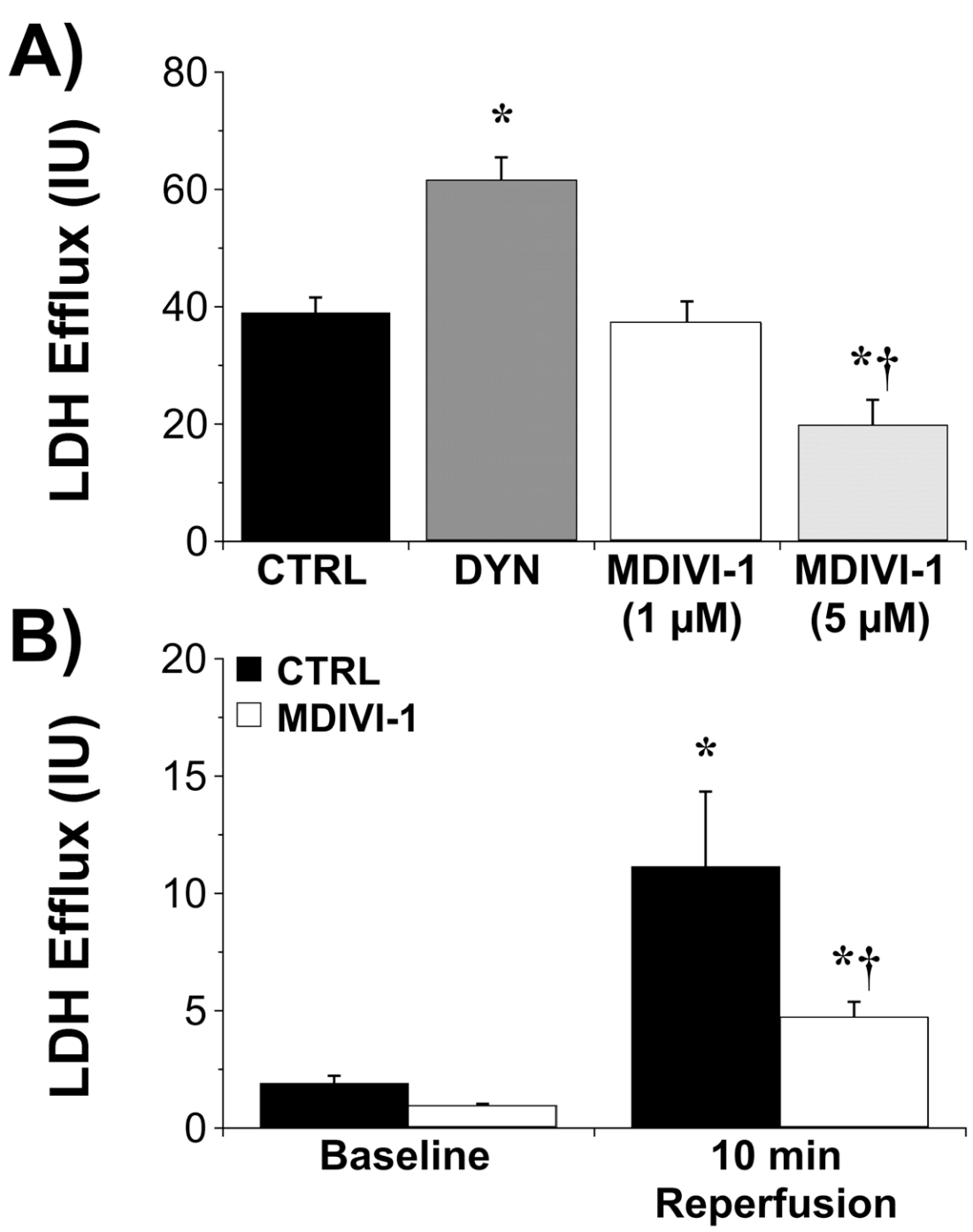

Fig. 4.

JPET Fast Forward. Published on November 8, 2019 as DOI: 10.1124/jpet.119.258897
This article has not been copyedited and formatted. The final version may differ from this version.

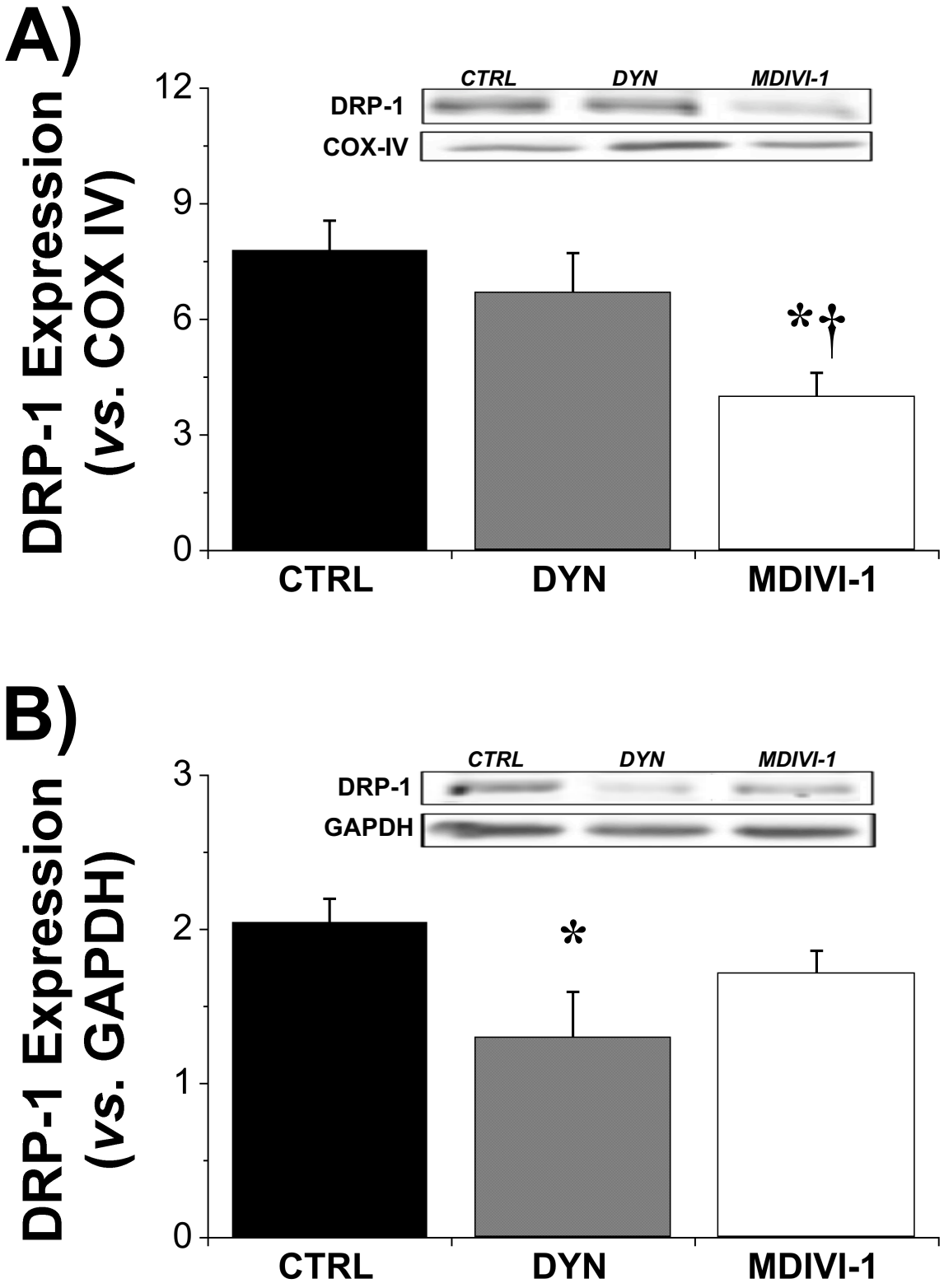

Fig. 5.

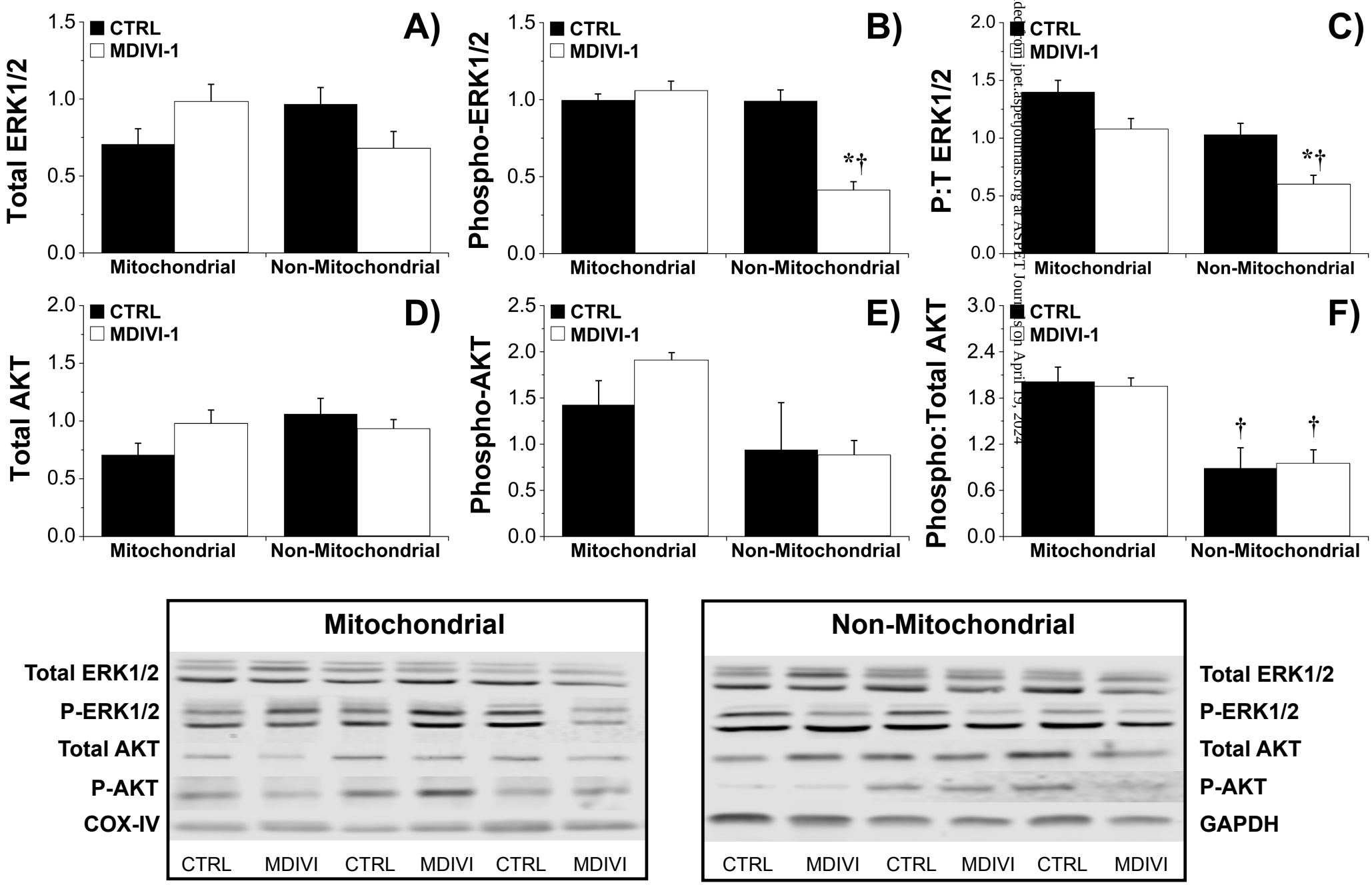

JPET Fast Forward. Published on November 8, 2019 as DOI: 10.1124/jpet.119.258897
This article has not been copyedited and formatted. The final version may differ from this version.

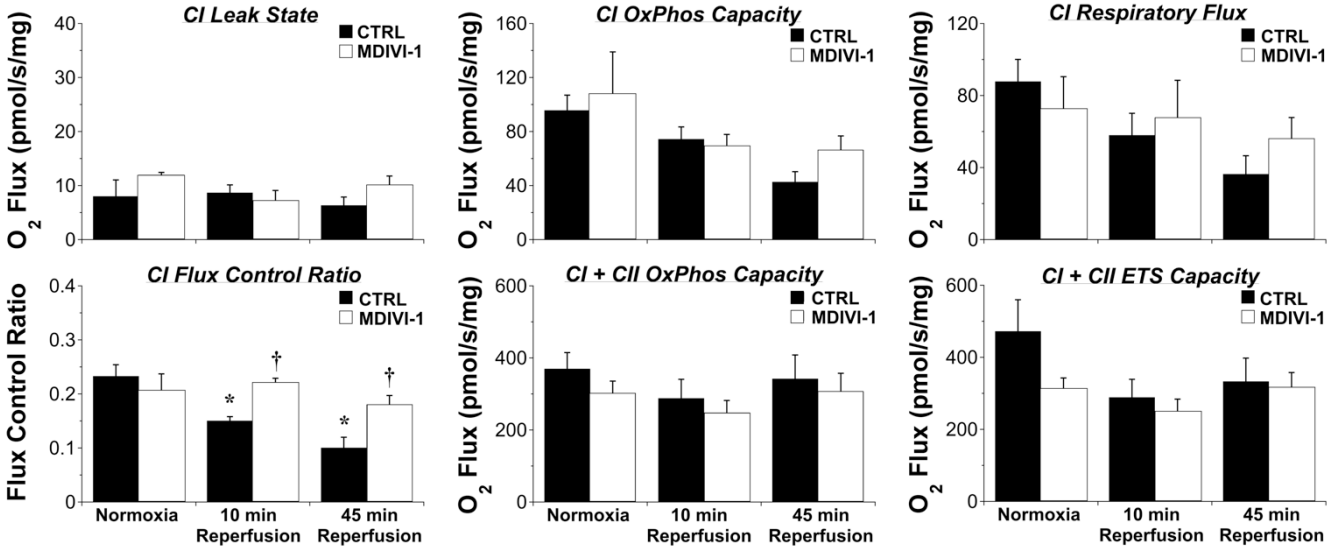

Fig. 7.

JPET Fast Forward. Published on November 8, 2019 as DOI: 10.1124/jpet.119.258897
This article has not been copyedited and formatted. The final version may differ from this version.

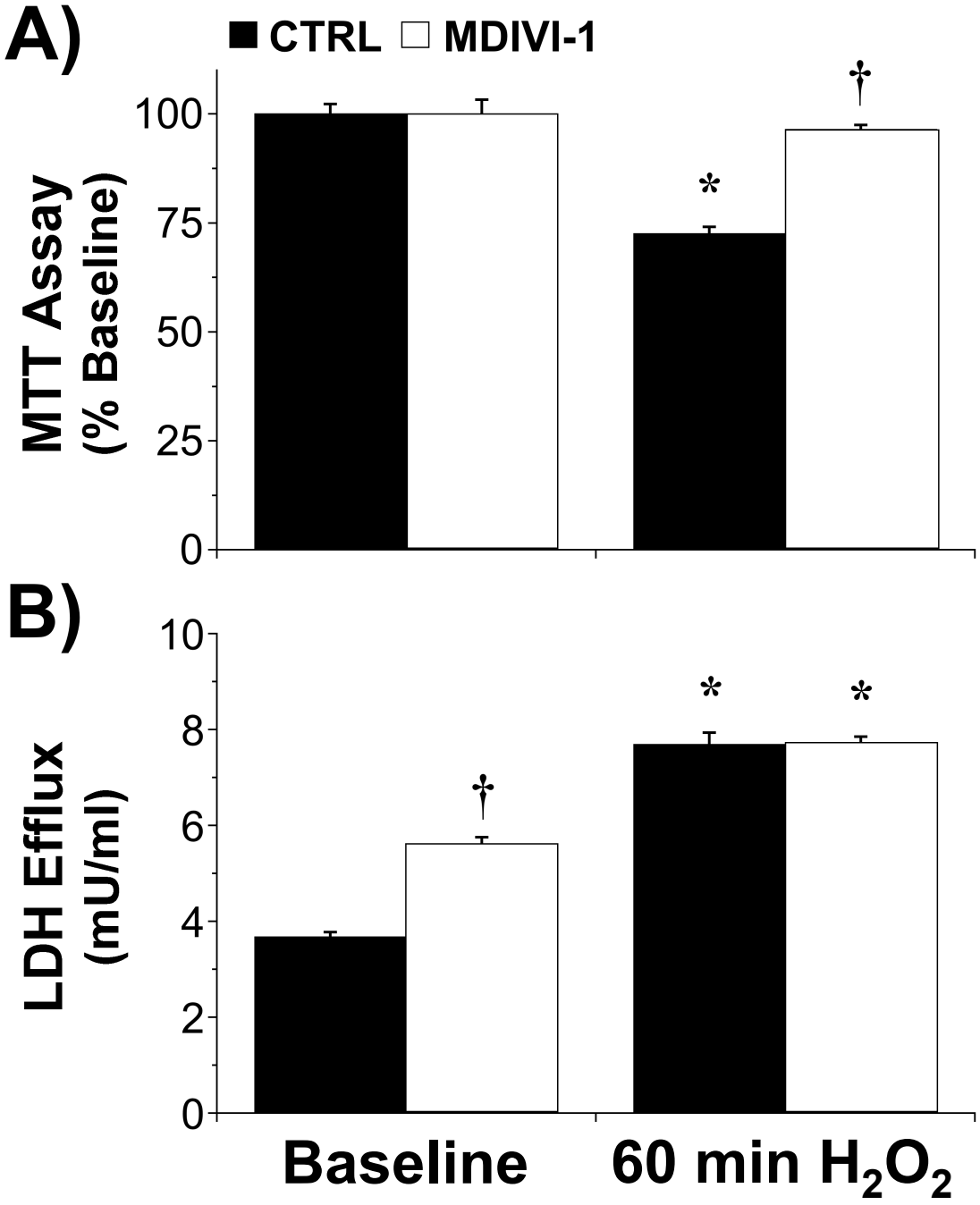

Fig. 8.

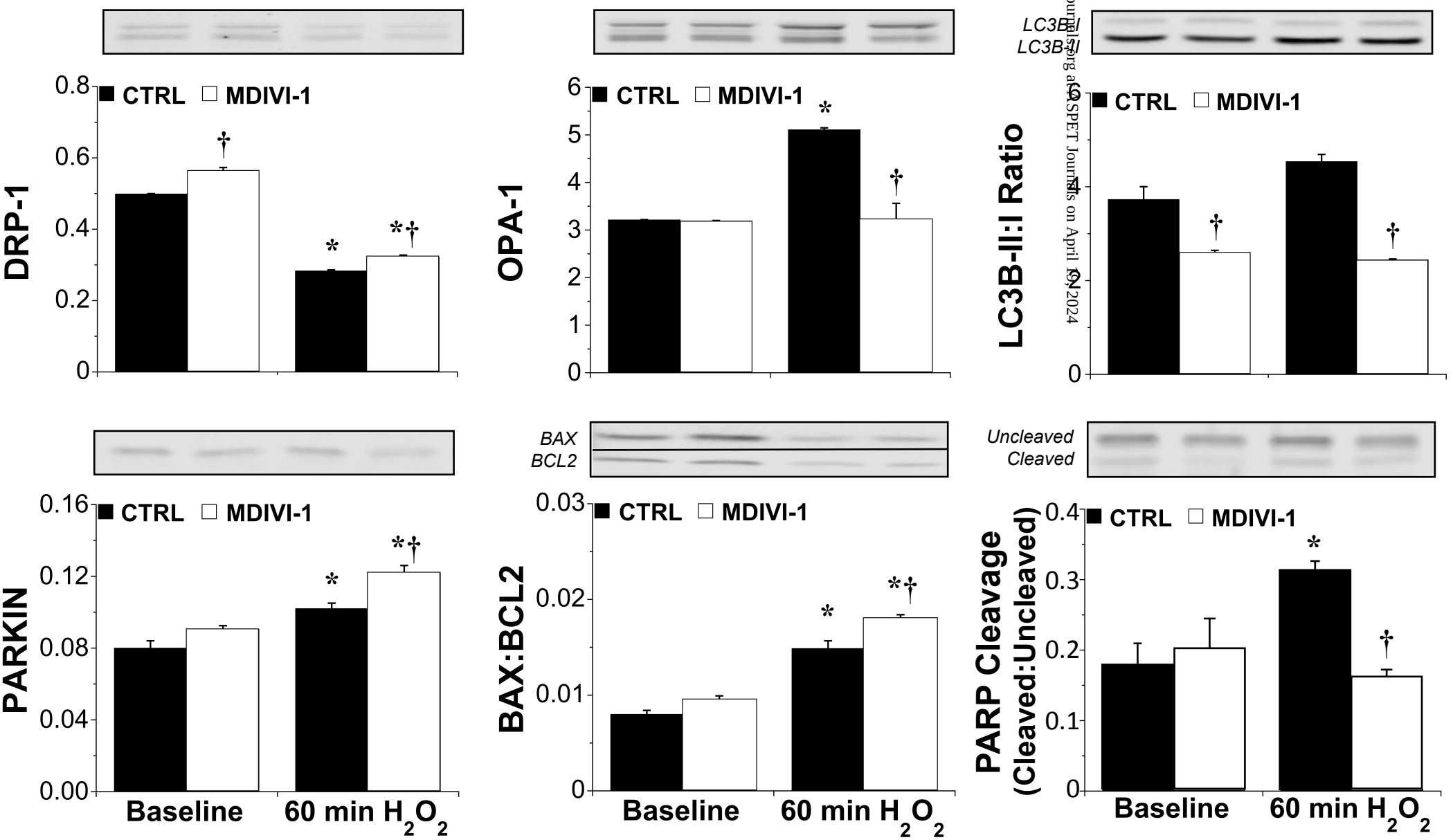

JPET Fast Forward. Published on November 8, 2019 as DOI: 10.1124/jpet.119.258897
This article has not been copyedited and formatted. The final version may differ from this version.

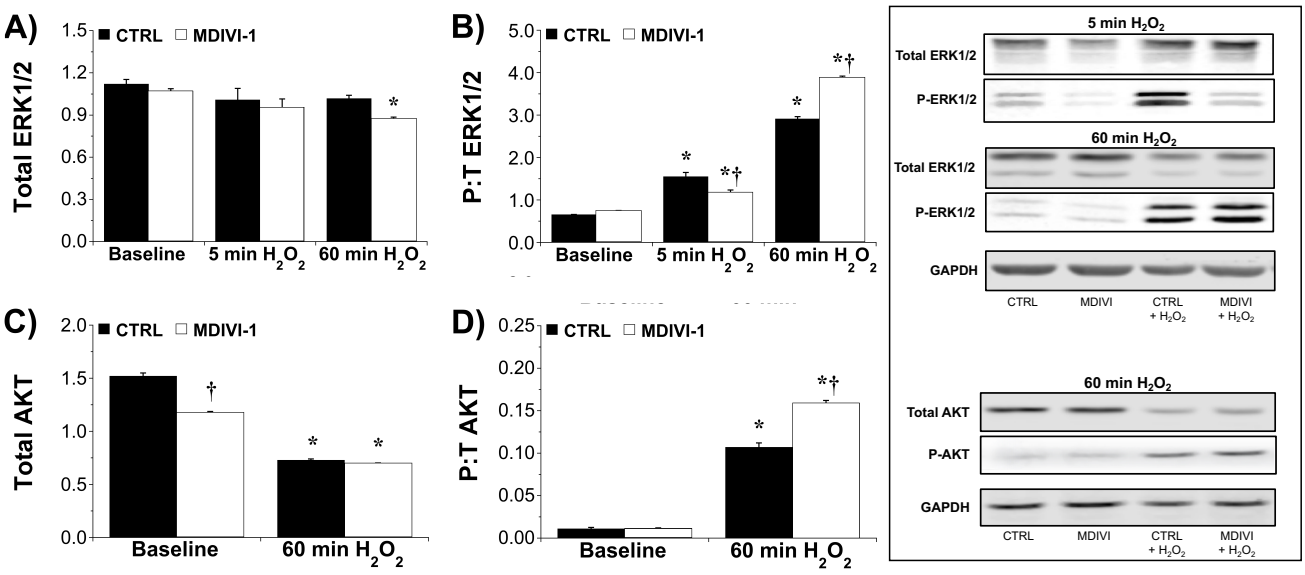

Fig. 10.

JPET Fast Forward. Published on November 8, 2019 as DOI: 10.1124/jpet.119.258897
This article has not been copyedited and formatted. The final version may differ from this version.

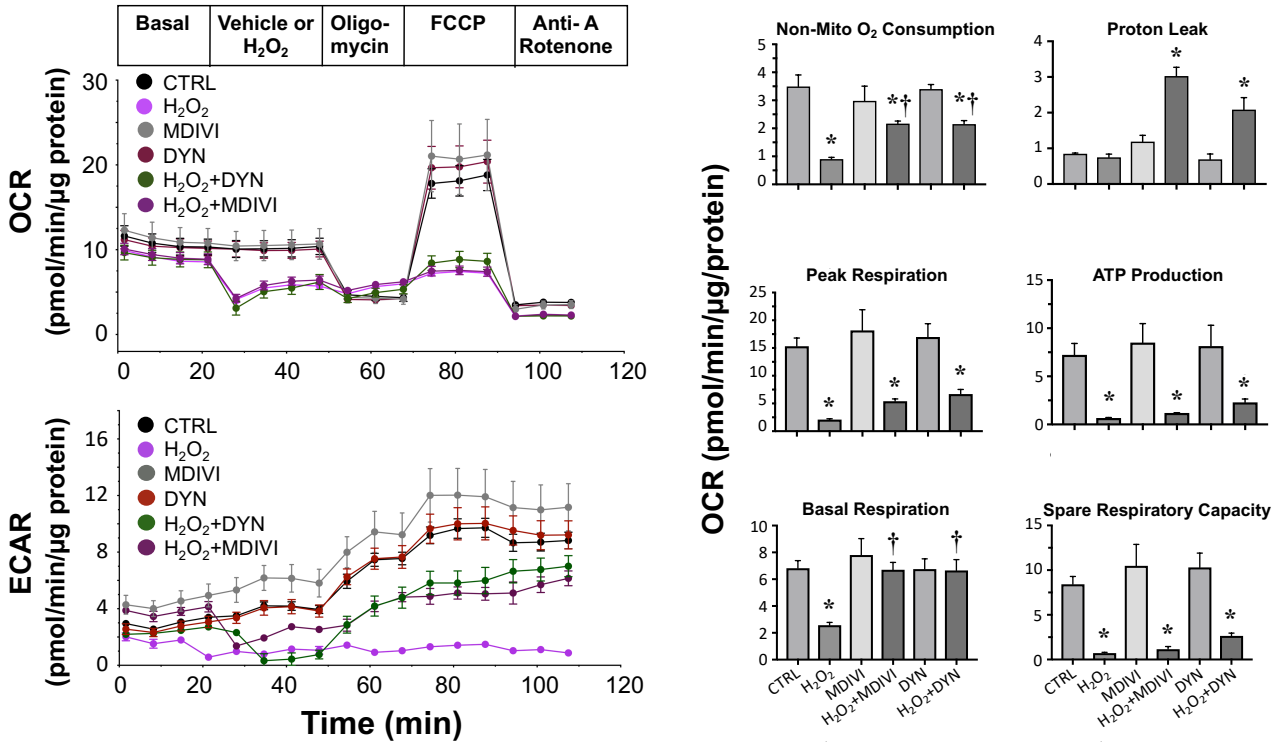

Fig. 11.

Lauren Wendt, Jelena Vider, Louise E. See Hoe, Eugene Du Toit, Jason N. Peart, John P. Headrick

Complex Effects of Putative DRP-1 Inhibitors on Stress Responses in Mouse Heart and Rat Cardiomyoblasts

The Journal of Pharmacology and Experimental Therapeutics

Supplemental Figures

Fig. 1

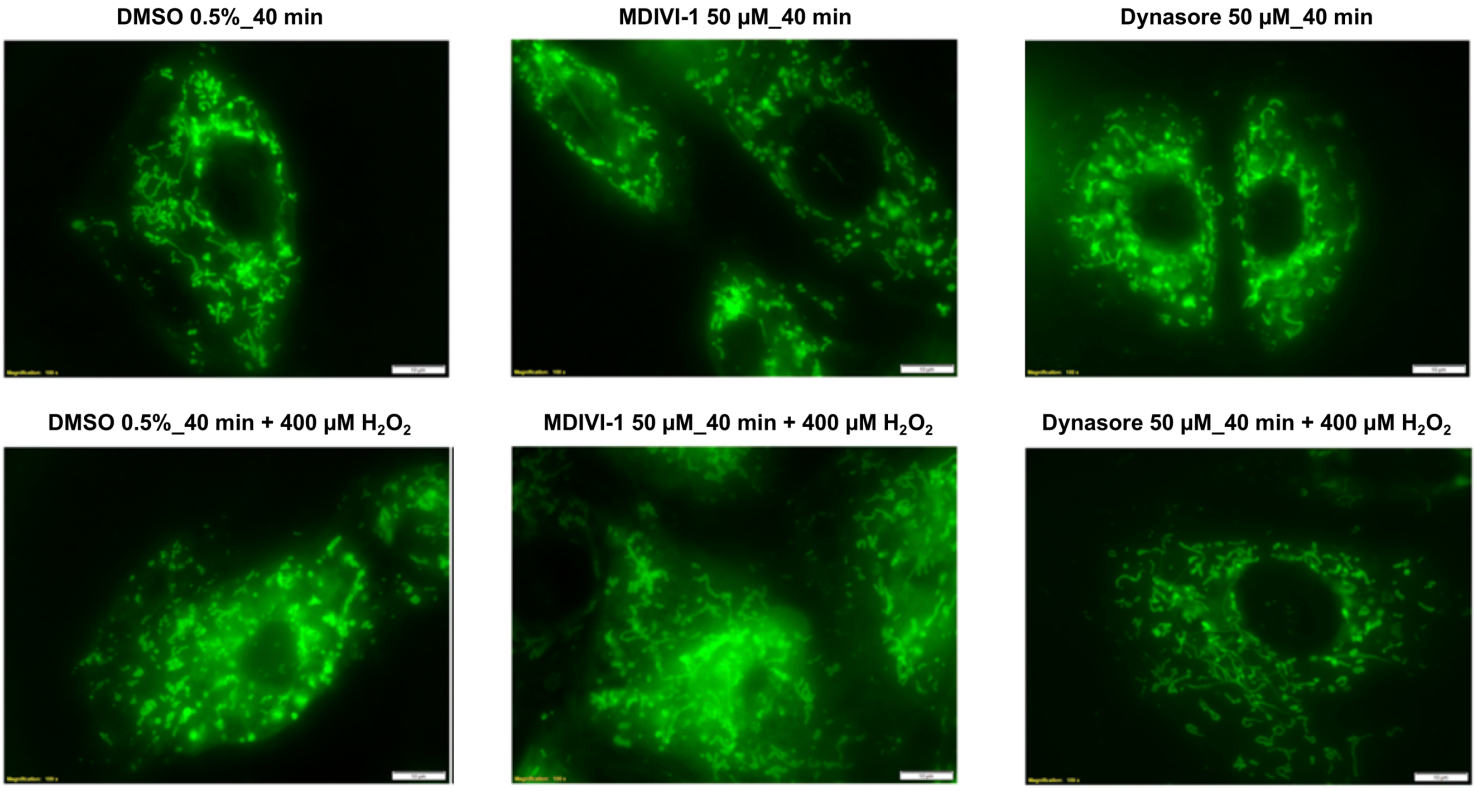

Mitochondrial morphology in H9c2 cardiomyoblasts exposed to H_2O_2 ± DRP-1 inhibitors. H9c2 cells were stained with 100 nM MitoTracker green (Thermo Fisher Scientific, Waltham, Massachusetts) in HBSS for 20 min at 37°C. After staining, HBSS was replaced for full media with 50 µM MDIVI/Dynasore or DMSO (0.5% final concentration) and incubated for 40 min. H_2O_2 was added to corresponding wells at 400 µM final concentration prior to imaging using fluorescence microscopy (CellM; Olympus, Japan). Note mitochondrial fragmentation (punctate staining) in H_2O_2 exposed cells, an effect limited by DRP-1 inhibitors.

Fig. 2

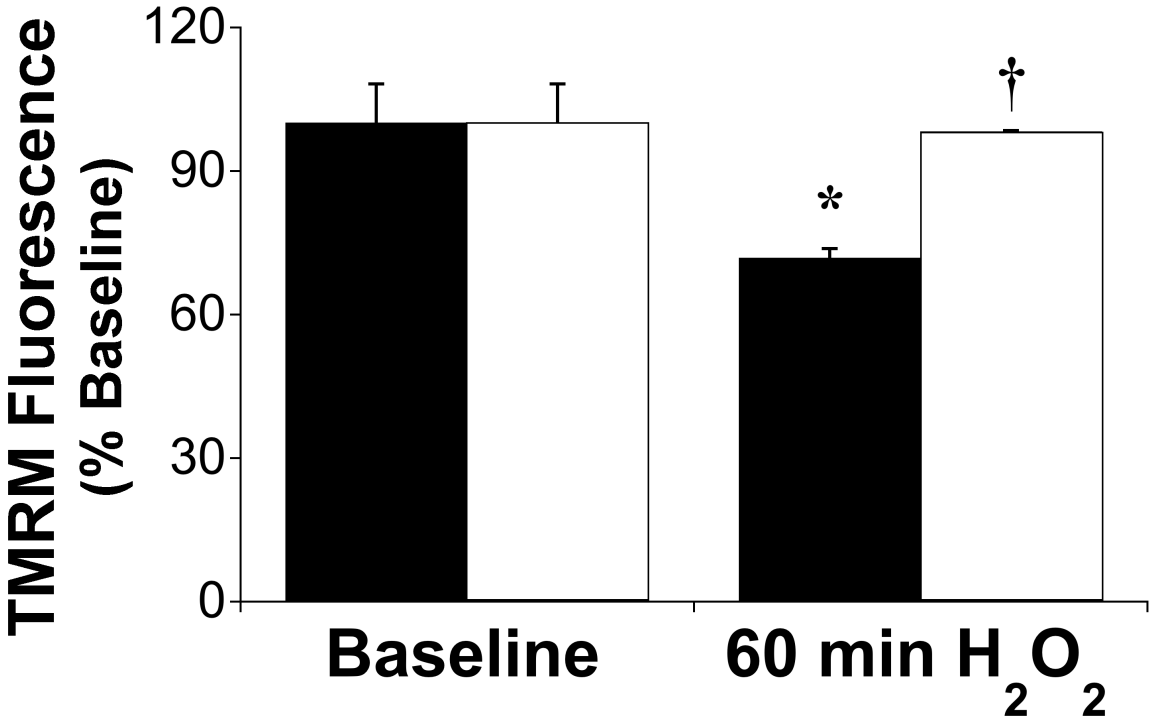

Preliminary analysis of mitochondrial membrane potential in H9c2 cardiomyoblasts exposed to H_2O_2 ± MDIVI-1. For assessment of mitochondrial membrane potential (Δψm) the fluorescent probe tetramethylrhodamine methyl ester perchlorate (TMRM) was employed, accumulating within mitochondria in proportion to Δψm. After experimentation cells were incubated with 100 μM TMRM for 20 min at 37°C (protected from light), harvested and re-suspended in PBS for analysis in a FACS-Calibur flow cytometer ((BD Bioscience, San Jose, CA, USA), with excitation at 549 nm and emission at 575 nm. Data were analyzed using FlowJo software, with median fluorescent intensity values calculated. Results suggest a ~20% fall in membrane potential with H_2O_2, an effect reversed by MDIVI-1, however it must be noted data were acquired with a potentially high quenching concentration (100 μM) of TMRM.

Fig. 3.

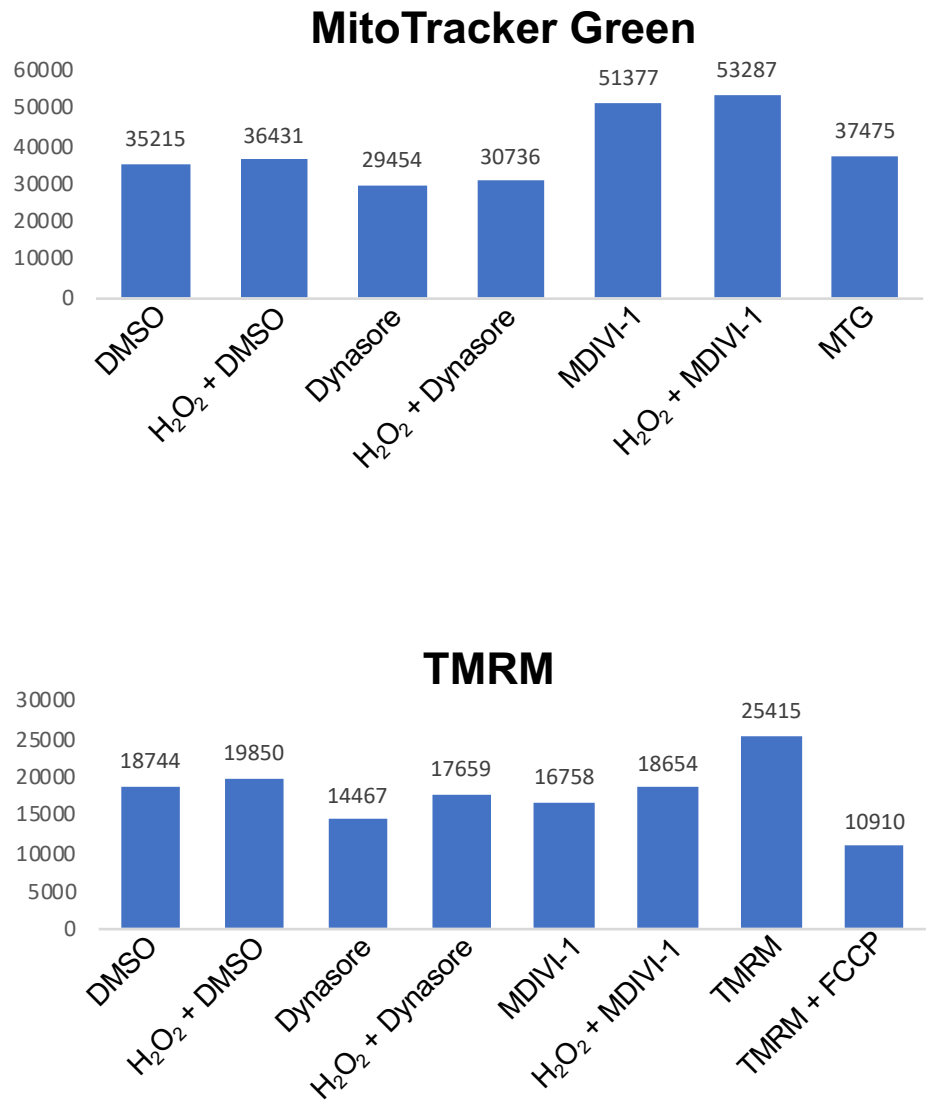

Supplementary flow cytometry data for MitoTracker green (MTG) and TMRM in H9c2 cardiomyoblasts exposed to H_2O_2 ± DRP-1 inhibitors. H9c2 cells were stained with 100 nM MitoTracker green (Thermo Fisher Scientific, Waltham, Massachusetts) in HBSS for 20 min at 37°C. After staining HBSS was replaced for full media with 50 µM MDIVI/Dynasore or DMSO (0.5% final concentration) and incubated for 40 min. After treatment cells were harvested and stained with 20 nM TMRM at 37°C (protected from light) in HBSS+2% FBS. H_2O_2 was added to corresponding tubes at 400 µM final concentration prior to analysis on a BD LSRII Fortessa flow cytometer (BD Bioscience, San Jose, CA, USA) with excitation at 561 nm, 88/12 BP. Data were analyzed using FlowJo software, with median fluorescent intensity values calculated. Note an apparent drop of mitochondrial potential with MDIVI/Dynasore treatment and increase in MitoTracker green MFI with MDIVI treatment.